JPET Fast Forward. Published on September 7, 2016 as DOI: 10.1124/jpet.116.236455
This article has not been copyedited and formatted. The final version may differ from this version.

JPET #236455

Revised

LPA_1 mediates antidepressant-induced ERK1/2 signalling and protection from oxidative stress in glial cells*

Maria C. Olianas, Simona Dedoni, Pierluigi Onali

Laboratory of Cellular and Molecular Pharmacology, Section of Neurosciences and Clinical Pharmacology, Department of Biomedical Sciences, University of Cagliari, Cagliari, Italy.

Running title: antidepressant signalling through LPA_1 in glial cells

Corresponding author: Dr. Pierluigi Onali, Laboratory of Cellular and Molecular Pharmacology, Section of Neurosciences and Clinical Pharmacology, Department of Biomedical Sciences, University of Cagliari, 09042 Monserrato (Ca), Italy.

Tel: +39-70-675-4321; Fax: +39-70-675-4320; E-mail: onali@unica.it

Number of text pages: 46

Number of tables: 0

Number of figures: 9

Number of references: 63

Number of words in Abstract:: 237

Number of words in Introduction: 606

Number of words in Discussion: 1373

Abbreviations: BDNF, brain-derived neurotrophic factor; CREB, cyclic AMP response element binding protein; DAPI, 4',6-diamidino-2phenylindole dihydrochloride; EGF, epidermal growth factor; EGF-R, EGF receptor; ERK1/2, extracellular signal-regulated protein kinases 1 and 2; FCS, foetal calf serum; FGF-2, basic fibroblast growth factor; FGF-R, FGF receptor; GAPDH, glyceraldehyde 3-phosphate dehydrogenase; GDNF, glial-derived growth factor; GPCRs, G protein-coupled receptors; 5-HT, 5-hydroxytryptamine; LPA, lysophosphatidic acid; MTT, 3-4(4,5-dimethyl-thiazol-2yl)-2,5-diphenyl-tetrazolium bromide; NBFI, norbinaltorphimine; PARP, poly (ADP-ribose) polymerase; PBS, phosphate buffered saline; PDGF-BB, platelet-derived growth factor-BB; PDGF-R, PDGF receptor β; PMSF, phenylmethylsulphonyl fluoride; PI3K, phosphoinositide 3-kinase; PTX, pertussis toxin; SDS, sodium dodecyl sulphate; siRNA, small interfering RNA.

Recommended section assignment: Neuropharmacology.

Abstract

Antidepressants have been shown to affect glial cell functions and intracellular signalling through mechanisms still not completely understood. In the present study, we provide evidence that in glial cells the lysophosphatidic acid (LPA) receptor LPA_1 mediates antidepressant-induced growth factor receptor transactivation, ERK1/2 signalling, and protection from oxidative stress. Thus, in C6 glioma cells and rat cortical astrocytes ERK1/2 activation induced by either amitriptyline or mianserin was antagonized by Ki16425 and VPC 12249 (S), which block LPA_1 and LPA_3 receptors, and by AM966, which selectively blocks LPA_1. Cell depletion of LPA_1 with siRNA treatment markedly reduced antidepressant- and LPA-induced ERK1/2 phosphorylation. LPA_1 blockade prevented antidepressant-induced phosphorylation of the transcription factors CREB and Elk-1. Antidepressants and LPA signalling to ERK1/2 was abrogated by cell treatment with pertussis toxin and by inhibition of fibroblast growth factor receptor (FGF-R) and platelet-derived growth factor receptor (PDGF-R) tyrosine kinases. Both Ki16425 and AM966 suppressed antidepressant-induced phosphorylation of FGF-R. Moreover, blockade of LPA_1 or inhibition of FGF-R and PDGF-R activities prevented antidepressant-stimulated Akt and GSK-3β phosphorylations. Mianserin protected C6 glioma cells and astrocytes from apoptotic cell death induced by H_2O_2, as indicated by increased cell viability, decreased expression of cleaved caspase 3, reduced cleavage of poly-ADP ribose polymerase and inhibition of DNA fragmentation. The protective effects of mianserin were antagonized by AM966. These data indicate that LPA_1 constitutes a novel molecular target of the regulatory actions of tricyclic and tetracyclic antidepressants in glial cells.

Introduction.

A growing body of evidence indicates that glial cells constitute a major cellular target of antidepressants (Czeh and Di Benedetto, 2013; Sanacora and Banasr, 2013). Animal studies have shown that *in vivo* repeated administration of antidepressants up-regulates the hippocampal expression of glial fibrillary acidic protein (GFAP), a major intermediate filament protein of astrocytes, and prevents or reverses the decrease in hippocampal GFAP induced by chronic stress (Sillaber et al, 2008; Liu et al., 2009). Animal treatment with antidepressants has also been demonstrated to affect the brain expression of other specific astroglial proteins, including the pro-apoptotic protein Ndrg2 (Nichols, 2003), the gap junction protein Connexin 43 (Fatemi et al., 2008), the glutamate transporter GLT1 (Reagan et al., 2004) and the calcium binding protein S100β (Manev et al., 2001). Many of these changes have been proposed to contribute to the therapeutic efficacy of antidepressants (Czeh and Di Benedetto, 2013; Sanacora and Banasr, 2013). Furthermore, a number of *in vitro* studies have documented that antidepressants can act directly on glial cells. In primary cultures of astrocytes and in rat C6 glioma cells, which retain several morphological and neurochemical properties of astrocytes (Bissel et al., 1974; Pfeiffer et al., 1970), distinct classes of antidepressants have been shown to induce the activation of the extracellular signal-regulated kinases 1 and 2 (ERK1/2) signalling pathway (Khawaja et al., 2004; Li et al., 2008), which plays a critical role in controlling cell differentiation and survival (Roux and Blenis, 2004), and is a putative key regulator of motivational and affective behaviour (Duric et al., 2010). In glial cells, antidepressant-induced ERK1/2 activation has been reported to mediate the phosphorylation/activation of the transcription factor CREB and the expression and

release of the neurotrophic factors brain-derived neurotrophic factor (BDNF) and glial-derived neurotrophic factor (GDNF) (Mercier et al., 2004; Hisaoka et al., 2007).

A major issue in understanding how antidepressants directly affect glial cell activity is the identification of the mechanisms by which these drugs can trigger intracellular signalling. Previous studies have reported that in glial cells distinct classes of antidepressants alter the subcellular localization of heterotrimeric G proteins (Donati and Rasenick, 2005), change the expression of β-arrestin 2 (Golan et al., 2010), and activate different receptor systems, including fibroblast growth factor (FGF) receptor (Hisaoka et al., 2011), $5HT_{2B}$ receptors (Li et al., 2008) and κ opioid receptors (Onali et al., 2010; Olianas et al., 2012). These studies suggest that antidepressants, besides inhibiting monoamine transporters in nerve terminals, possess the ability to affect different signalling molecules in glial cells.

The bioactive phospholipid lysophosphatidic acid (LPA), which acts as endogenous agonist at six distinct G protein coupled receptors (GPCRs) termed LPA_{1-6} (Yung et al., 2015), is known to exert a variety of effects on astrocytes, including regulation of cell morphology, mitogenesis, expression of neurotrophic genes, and production of neuronal-differentiating factors (Ramakers and Moolenaar, 1998; Tabuchi et al., 2000; Spohr et al., 2008; Sato et al., 2011). We have recently observed that in CHO-K1 fibroblasts different antidepressants induce insulin-like growth factor-1 receptor transactivation, ERK1/2 signalling and enhanced cell proliferation through the LPA_1 receptor (Olianas et al., 2015). This observation indicated that LPA_1 participates in the cellular actions of antidepressants and prompted us to investigate whether this receptor system could be involved in the regulation of glial cell activity by these drugs.

In the present study, we show that in C6 glioma cells and primary cultures of rat cortical astrocytes LPA_1 mediates the growth factor receptor transactivation and stimulation of ERK1/2 signalling by the tricyclic antidepressant amitriptyline and the tetracyclic antidepressant mianserin. Moreover, we show that mianserin protects glial cells from oxidative stress-induced apoptosis and that this effect is dependent on LPA_1.

Materials and Methods

Materials

Amitriptyline hydrochloride, nortriptyline hydrochloride, imipramine hydrochloride, desipramine hydrochloride, mianserin hydrochloride, mirtazapine hydrochloride, clomipramine hydrochloride, *Bordetella* pertussis toxin (PTX). recombinant human platelet-derived growth factor-BB (PDGF-BB), 3-4(4,5-dimethyl-thiazol-2yl)-2,5-diphenyl-tetrazolium bromide (MTT), 4',6-diamidino-2phenylindole dihydrochloride (DAPI), and 5-hydroxytryptamine hydrochloride (5-HT) were from Sigma-Aldrich (St. Louis, MO, USA). Recombinant human EGF was from Cell Signaling Technology (Danvers, MA, USA). Ki16425 (3-(4-[4-([1-(2-chlorophenyl)ethoxy]carbonyl amino)-3-methyl-5-isoxazolyl) propanoic acid), PD173074 (N-[2-[[4-(diethylamino)butyl]amino]-6-(3,5-dimethoxyphenyl)pyrido[2,3-d]pyrimidin-7-yl]-N-(1,1-dimethylurea) and norbinaltorphimine dihydrochloride (NBFI) were obtained from Santa Cruz Biotechnology (Dallas, TX, USA). AM966 (4'-{4-[(R)-1-(2-chloro-phenyl)-ethoxycarbonylamino]-3-methyl-isoxazol-5-yl}-biphenyl-4yl)-acetic acid was from Chem Scene (Monmouth Junction, NJ, USA). VPC12249 (S) ((S)-phosphoric acid mono-[3-(4-benzyloxy-phenyl)-2-octadec-9-enoylamino-propyl] ester ammonium salt)

was from Avanti Polar Lipids Inc. (Alabaster, AL, USA). 1-Oleoyl-lysophosphatidic acid (LPA) was from either Santa Cruz Biotechnology or Sigma-Aldrich. Tyrphostin AG1296 was from Merck/Millipore (Darmstadt, Germany). H2L5186303 ((Z,Z)-4-4'-[1,3-phenylenebis(oxy-4,1-phenyleneimino)]bis-4-oxo-2-butenoic acid) was from Tocris Bioscience (Bristol, UK). Recombinant mouse basic FGF (FGF-2) was from ProSpec-Tany TechnoGene Ltd (Ness Ziona, Israel).

Cell culture

C6 rat glioma cells (European Collection of Cell Cultures, Porton Down, Wiltshire, UK) were grown in Ham's F-12 medium containing 2 mM L-glutamine, 10 % foetal calf serum (FCS) and 0.5 % penicillin/streptomycin (P/S) in a humidified 95 % air and 5 % CO_2 at 37 °C.

Primary cultures of astrocytes were prepared from the cerebral cortex of newborn (1 day old) Sprague-Dawley rats. Experiments were performed in accordance with the European Communities Council Directive (86/609EEC) and the Principles of Laboratory Animal Care in Italy. Following removal of meninges, the brain tissue was minced into small pieces and incubated in cell dissociation buffer (Invitrogen/Life Technologies, Monza, Italy) containing 0.2 % trypsin for 20 min at 37 °C. Soyabean trypsin inhibitor and Dnase I (Sigma Aldrich) were then added and the incubation was continued for 5 min. Cells were dissociated by aspiration through fire-polished Pasteur pipettes, collected by centrifugation and resuspended in DMEM-Ham's F-12 medium containing 10 % FCS and 0.5 % P/S. Cells were seeded into 75-cm^2 flasks and incubated at 37 °C in an atmosphere with 5 % CO_2. Following incubation for 2 weeks, astrocytes were collected by shaking the cultures at 350 rpm overnight at 37 °C (McCarty and DeVellis, 1980). Astrocytes were grown in DMEM-Ham's F-12

JPET Fast Forward. Published on September 7, 2016 as DOI: 10.1124/jpet.116.236455
This article has not been copyedited and formatted. The final version may differ from this version.

medium supplemented with 10 % FCS and 0.5 % P/S at 37 °C in an atmosphere with 5 % CO_2. Cultured cells displayed a flat and polygonal morphology typical of type I astrocytes (Raff et al., 1983). Immunofluorescence analysis indicated that the cells were > 95 % positive by immunofluorescence staining with an anti-GFAP antibody (Sigma-Aldrich). Cells were used 3-4 days after replating.

Small interfering RNA (siRNA) transfection

C6 glioma cells were transfected with either control siRNA-A or mouse LPA_1 siRNA (Santa Cruz Biotechnology) using Lipofectamine RNAiMAX (Invitrogen/Life Technologies) as transfection reagent. Cells were incubated with siRNA duplexes (75 nM) for 12 h at 37 °C and analyzed 48 h post-transfection. To determine transfection efficiency, parallel samples were treated with fluorescein-conjugated control siRNA-A (Santa Cruz Biotechnology). An efficiency of ~ 60 % was obtained in three separate experiments.

Preparation of crude plasma membrane fraction

C6 glioma cells grown to confluency in 100 mm Petri dishes were washed, scraped into ice-cold PBS and centrifuged at 1000 rpm at 4 °C. Cells were washed twice with PBS and the final pellet was stored at -80 °C for 24 h. The frozen cells were thawed and resuspended in ice-cold 10 mM HEPES/NaOH (pH 7.40) containing 0.1 mM EDTA, 4 mM sodium pyrophosphate, 2 mM sodium orthovanadate, 10 mM sodium fluoride, 0.1 % phosphatase inhibitor cocktail 3, 1 % protease inhibitor cocktail and 1 mM phenylmethylsulphonyl fluoride (PMSF) (HEPES/EDTA buffer). Cells were lysed by using a glass/glass Dounce tissue grinder (pestle A) and the homogenate was centrifuged for 10 min at 500 g at 4 °C. The supernatant was collected and centrifuged at 48,000 g for 10 min at °4 C. The supernatant was discarded and the

pellet was resuspended in ice-cold HEPES/EDTA buffer and centrifuged at 48,000 g for 10 min at °4C. The final pellet was resuspended in ice-cold buffer containing phosphate-buffered saline (PBS), 0.1 % sodium dodecyl sulphate (SDS), 1 % Nonidet P-40, 0.5 % sodium deoxycholate, 2 mM EDTA, 2 mM EGTA, 4 mM sodium pyrophosphate, 2 mM sodium orthovanadate, 10 mM sodium fluoride, 20 nM okadaic acid, 0.1 % phosphatase inhibitor cocktail 3, 1 % protease inhibitor cocktail and 1 mM phenylmethylsulphonyl fluoride (PMSF) (RIPA buffer) supplemented with 0.1 % Triton X-100 and sonicated for 5 s before Western blot analysis.

Western blot analysis

Cells were serum-starved for 24 h, incubated in fresh serum-free medium for 1 h at 37 °C and then treated with the test agents as specified in the text. Cell extracts were prepared by scraping the cells in ice-cold RIPA buffer followed by sonication for 5 s. Aliquots of cell extracts were taken for protein determination by the Bio-Rad protein assay (Bio-Rad Lab., Hercules, CA, USA). Cell proteins were separated by SDS-polyacrylamide gel electrophoresis and then electrophoretically transferred to either polyvinylidene difluoride or nitrocellulose membranes. Membranes were incubated overnight at 4 °C with one of the following primary antibodies: anti-phospho-ERK1 (Thr202/Tyr204) / ERK2(Thr185/Tyr187) (RA 15002) (1:15,000) (Neuromics, Northfield, MN, USA); anti-ERK1/2 (#9102) (1:1000), anti-phospho-cyclic AMP responsive element binding protein (CREB) (Ser133) (#9191) (1:2000), anti-CREB (#9197) (1:1000), anti-phospho-ElK-1(Ser383) (#9181) (1:1000), anti-phospho-Akt (Thr308) (#2965), anti-phospho-glycogen synthase kinase-3β (GSK-3β) (Ser9) (#5558) (1:1000), anti-phospho-FGF receptor (Tyr653/654) (#3476) (1:1000), anti-phospho-PDGF receptor β (Tyr751) (#3166) (1:1000), anti-PDGF receptor β (#3175)

JPET Fast Forward. Published on September 7, 2016 as DOI: 10.1124/jpet.116.236455
This article has not been copyedited and formatted. The final version may differ from this version.

(1:1000), anti-cleaved poly-(ADP ribose) polymerase (PARP) (Asp214) (#9625) (1:1000), anti-PARP (#9542) (1:1000), anti-pan-cadherin (1.2000) (#28E12) (Cell Signaling Technology); anti-Akt (sc-8312) (1:1000), anti-GSK-3β (sc-9166) (1:1000), anti-LPA_1 (sc-515665) (1:2000) (Santa Cruz Biotechnology); anti-LPA_2 (ALR-032) (1:500) and anti-LPA_3 (ALR-033) (1:500) (Alomone Labs., Jerusalem, Israel); anti-FGF receptor 1 (bs-0230R) (1:1000) (Bioss, Inc., Woburn, MA, USA); anti-actin (A2066) (1:2000) (Sigma-Aldrich); anti-glyceraldehyde 3-phosphate dehydrogenase (GAPDH) (# 247002g) (1:5000) (Synaptic Systems, Gottingen, Germany). Following incubation with horseradish peroxidase-conjugated secondary antibodies, immunoreactive bands were detected by using ECL Plus and ECL Hyperfilm (Amersham). The size of immunoreactive bands was determined by using molecular weight standards detected with an ECL suitable antibody (Santa Cruz) and Sharp Mass V Plus pre-stained protein molecular weight marker (EuroClone, Milan, Italy). Band densities were determined by densitometric analysis using Image Scanner III (GE Healthcare, Milan, Italy) and NIH ImageJ software (US National Institutes of Health, Bethesda, MA, USA). The optical density of phosphoproteins was normalized to the density of the corresponding total protein in the same samples. For analysis of cleaved PARP the formation of the cleaved protein was normalized to the level of the uncleaved form determined in the same samples. For the other proteins, the densitometric values were normalized to the levels of either actin or GAPDH.

Immunofluorescence analysis

Cells plated on poly-L-lysine-pre-coated glass coverslips were serum-starved and treated with the test compounds at 37 °C as specified in the text. Following fixation with 4 % paraformaldehyde and permeabilization with 0.2 % Triton X-100, the cells

JPET Fast Forward. Published on September 7, 2016 as DOI: 10.1124/jpet.116.236455
This article has not been copyedited and formatted. The final version may differ from this version.

were blocked with 3 % BSA and 1 % normal goat serum and incubated overnight at 4 °C with either anti-phospho-CREB (Ser133) antibody (#06-519) (1:1000) (Upstate Biotechnology Inc., Lake Placid, NY, USA) or anti-cleaved caspase 3 (Asp175) (#9664) (1:200) (Cell Signaling Technology). Control samples were incubated in the absence of primary antibodies. After rinsing, the cells were incubated with Alexa 488-conjugated goat IgG (Invitrogen-Molecular Probes). Cell nuclei were stained with 0.1 µg/ml DAPI. Images were captured at constant camera settings and analyzed using the program Cell P (Olympus Soft Imaging Solutions, Hamburg, Germany) as previously described (Olianas et al., 2008). No labeling was detected in samples treated without primary antibodies. Four separate culture preparations were analyzed by an investigator unaware of the treatment.

Terminal transferase dUTP nick end-labeling (TUNEL) assay

Cultured astrocytes grown on glass coverslips were treated with the test compounds at 37 °C as specified in the text. In situ TUNEL assay was performed using the DeadEnd fluorimetric TUNEL system (Promega, Madison, WI, USA), according to the manufacturer's instructions. Cell nuclei were stained with DAPI. Images were captured over randomly selected fields and analyzed with Cell P software as described for immunofluorescence assays. Three separate culture preparations were analyzed by an investigator unaware of the treatment.

Cell viability analysis

Cell viability of C6 glioma cells was determined by fluorescence-based analysis using the Muse Cell Count and Viability kit provided by Millipore (Temecula, CA, USA). Briefly, serum-starved cells were exposed to the experimental agents for the indicated times in serum-free medium, detached by trypsin/EDTA treatment, washed

in medium containing 10 % FCS and incubated with the assay reagent solutions for 5-15 min as specified by the manufacturer's protocol. Cells were then analyzed by using the Muse Cell Analyzer (Millipore).

Cell viability of rat astrocytes was performed by MTT assay in a 96-well plate. Serum-starved astrocytes were treated with the experimental agents as specified in the text After washing with PBS, the cells were incubated for 3 h at 37 °C with MTT (0.5 mg/ml) dissolved in PBS and filtered through a 0.20 µm Millipore filter. The blue formazan product was solubilised by the addition of 10 % SDS in 10 mM HCl. Absorbance was measured on a Wallach Victor microplate reader (PerkinElmer, Waltham, MA, USA) using a reference wavelength of 630 nm and a test wavelength of 530 nm.

Experiments were conducted to establish the concentrations of freshly prepared hydrogen peroxide (H_2O_2) and the incubation times that produced no more than 50 % cell death in both C6 glioma cells and rat cortical astrocytes.

Statistical analysis

Results are reported as mean ± SEM of N independent experiments. Concentration-response curves were analyzed by the program Graph Pad Prism (San Diego, CA, USA.), which yielded the drug concentration producing half-maximal stimulation (EC_{50}) or half-maximal inhibition (IC_{50}), and maximal effect (E_{max}). Values of experimental groups were routinely expressed as a percent or fold stimulation of control, which was included in each independent experiment. The control was set as 100 or 1 with a variance obtained by expressing each control value as a ratio or percent of the mean of the raw values of the control group**.** Statistical analysis was performed by either unpaired Student's t test or one-way analysis of variance

JPET Fast Forward. Published on September 7, 2016 as DOI: 10.1124/jpet.116.236455
This article has not been copyedited and formatted. The final version may differ from this version.

(ANOVA) followed by Newman-Keuls *post ho*c test as appropriate. A value of $P < 0.05$ was considered to be statistically significant.

Results

Stimulation of ERK1/2 phosphorylation by amitriptyline, mianserin and LPA in C6 glioma cells

Exposure of C6 glioma cells to either amitriptyline (15 µM) or mianserin (5 µM) for different periods of time showed that both drugs induced a rapid increase of ERK1/2 dual phosphorylation, which is an index of the kinase activation, without changing total ERK1/2 levels. In the presence of these drugs phospho-ERK1/2 levels increased about 4-fold (N = 4) at 10 min and then declined remaining above basal for at least 3 h (Fig.1A, B). Under the same experimental conditions, ERK1/2 phosphorylation induced by LPA (100 nM) showed a similar kinetic profile, being high at 10 min and slowly decreasing at later time points (Fig. 1C).

The stimulations of ERK1/2 phosphorylation elicited by amitriptyline and mianserin were concentration-dependent with EC_{50} values of 2.1 ± 0.5 and 1.2 ± 0.3 µM, respectively, and E_{max} values corresponding to 4.2- ± 0.7 and 4.7- ± 0.8 fold increase of basal value (N = 5 , $P < 0.001$), respectively (Fig. 1D,E). LPA also displayed a concentration-dependent stimulation of ERK1/2 with an EC_{50} of 260 ± 30 nM and E_{max} value of 9.4- ± 1.0 fold increase of basal value (N = 5, $P < 0.001$) (Fig. 1F).

LPA_1 antagonists inhibit ERK1/2 phosphorylation induced by amitriptyline and mianserin

As shown in Fig. 2A, preincubation of C6 glioma cells with either 1 µM Ki16425, which antagonizes LPA_1 and LPA_3 and has no activity at the other LPA receptors

(Ohta et al., 2003; Yanagida et al., 2009; Jiang et al., 2013), or 1 μM AM966, which preferentially blocks LPA_1 (Swaney et al., 2010), completely prevented ERK1/2 stimulation induced by 100 nM LPA. Ki16425 (100 nM) and AM966 (100 nM) reduced the stimulatory effect elicited by amitriptyline (15 μM) by 84 ± 2 and 74 ± 3 %, respectively, (Fig. 2B) and that induced by mianserin (5 μM) by 80 ± 3 and 76 ± 4 %, respectively (Fig. 2C). Cell treatment with the LPA analog VPC12249 (S) (10 μM), which blocks LPA_1 and LPA_3 (Heise et al., 2001) reduced amitriptyline- and mianserin-stimulated ERK1/2 phosphorylation by 68 ± 4 and 70 ± 3 %, respectively (Fig. 2D). At the concentrations used, none of the antagonists affected the phosphorylation state of ERK1/2 *per se*.

Acute exposure of rat cortical astrocytes to LPA (1 μM) increased ERK1/2 phosphorylation by approximately 2.3-fold ($P < 0.001$, N = 10) (Fig. 2E). Cell pre-treatment with AM966 (1 μM) completely blocked the stimulatory effect of LPA, whereas Ki16425 (1 μM) curtailed the response by 80 % ($P < 0.01$) (Fig 2E). In these cells, amitriptyline (15 μM) and mianserin (5 μM) stimulated ERK1/2 phosphorylation by about 2-fold ($P < 0.001$, N = 12). The stimulatory effect elicited by both antidepressants was significantly reduced by cell pre-treatment with either Ki16425, AM966 or VPC12249 (S) (Fig. 2F-H).

Concentration-response curves performed in C6 glioma cells indicated that AM966 and Ki16425 completely suppressed LPA (1 μM)-induced ERK1/2 phosphorylation with IC_{50} values of 13.8 ± 1.2 and 63.5 ± 9 nM, respectively (Fig. 3A,B). The stimulatory effect of amitriptyline (15 μM) was antagonized by AM966 and Ki16425 with IC_{50} values of 1.0 ± 0.2 and 2.8 ± 0.5 nM, respectively, and maximal inhibitory effects of 83 and 76 %, respectively (Fig 3C, D). Similarly, the stimulatory effect of

JPET Fast Forward. Published on September 7, 2016 as DOI: 10.1124/jpet.116.236455
This article has not been copyedited and formatted. The final version may differ from this version.

mianserin (5 μM) was antagonized by either AM966 (IC_{50} = 1.6 ± 0.3 nM) or Ki16425 (IC_{50} = 3.2 ± 0.4 nM) with curves that reached a plateau at approximately 80 % inhibition (Fig. 3E, F). The compound H2L5186303, which displays selectivity for LPA_2 over LPA_1 and LPA_3 (Fells et al., 2008), had no effect on LPA (1 μM) stimulation of ERK1/2 at concentrations up to 1 μM (Fig. 3G). This antagonist also had no effect on the stimulatory responses elicited by either amitriptyline or mianserin (Fig. 3H).

We have previously reported that in rat C6 glioma cells amitriptyline and mianserin stimulated ERK1/2 phosphorylation by activating endogenous κ-opioid receptors (Onali et al., 2010; Olianas et al., 2012). To examine whether the incomplete blockade observed with AM966 and Ki16425 was due to the concomitant stimulation of κ-opioid receptors, cells were co-treated with the κ-opioid receptor antagonist nor-binaltorphimine (NBFI). As shown in Supplemental Figure 1, the combination of NBFI (100 nM) with Ki16425 (1 μM) completely blocked the stimulatory effect of amitriptyline (15 μM) and mianserin (5 μM).

LPA_1 knockdown inhibits antidepressant-induced ERK1/2 phosphorylation in C6 glioma cells

Western blot analysis of C6 glioma cell lysates with an antibody directed against the extracellular domain of LPA_1 detected the presence of a prominent immunoreactive band of ~ 41 kDa, which corresponds to the molecular mass of LPA_1 (Fig. 4A). Immunoblot analysis using antibodies against the extracellular domains of LPA_2 and LPA_3 also showed the presence of immunoreactive bands corresponding to LPA_2 (37 kDa) and LPA_3 (~41 kDa) (Fig. 4A). A similar pattern of receptor expression was observed when a crude plasma membrane preparation was examined (Fig. 4A).

JPET Fast Forward. Published on September 7, 2016 as DOI: 10.1124/jpet.116.236455
This article has not been copyedited and formatted. The final version may differ from this version.

Treatment of C6 glioma cells with LPA_1-siRNA reduced the expression levels of LPA_1 by 60 ± 5 % ($P < 0.001$), as compared to control siRNA-treated cells, but failed to significantly affect the expression levels of either LPA_2 or LPA_3 (Fig. 4B).

In cells depleted of LPA_1, ERK1/2 phosphorylation elicited by either amitriptyline (15 μM) or mianserin (5 μM) was reduced by 82 ± 3 and 80 ± 4 %, respectively, as compared with the responses observed in control siRNA-treated cells (Fig. 4C). Similarly, LPA_1-siRNA treatment reduced the stimulations induced by imipramine (15 μM) and LPA (50 nM) by 70 ± 2 and 74 ± 5 %, respectively (Fig. 4D).

Ki16425 and AM966 block the phosphorylation of CREB and ElK-1 induced by amitriptyline and mianserin

The transcription factor CREB is activated by phosphorylation at Ser133 in response to growth factors and a variety of extracellular stimuli acting through different protein kinase pathways, including ERK1/2 (Lonze and Ginty, 2002). Immunofluorescence analysis showed that exposure of C6 glioma cells to amitriptyline (15 μM) for 30 min induced a significant increase in the number of cell nuclei expressing phospho-Ser133-CREB (Fig. 5A). The increase was blocked by pre-treatment with Ki16425 (100 nM). Western blot analysis showed that in both C6 glioma cells and rat cortical astrocytes amitriptyline (15 μM) and mianserin (5 μM) increased phospho-CREB levels and this response was antagonized by AM966 (100 nM) (Fig. 5B,C).

Elk-1 is a transcription factor that is directly phosphorylated at Ser383 and Ser389 by ERK1/2 (Besnard et al., 2011). As shown in Fig. 5D, exposure of C6 glioma cells to either amitriptyline (15 μM) or mianserin (5 μM) induced a significant increase in the levels of phospho-Ser383-ElK-1, and this response was abrogated by pre-incubation with AM966 (100 nM).

JPET Fast Forward. Published on September 7, 2016 as DOI: 10.1124/jpet.116.236455
This article has not been copyedited and formatted. The final version may differ from this version.

PTX prevents antidepressant-induced ERK1/2 phosphorylation

In a number of cell types, LPA_1 has been shown to signal by coupling to distinct families of heterotrimeric G proteins, including $G_{i/o}$, $G_{q/11}$ and $G_{12/13}$ (Yung et al., 2015). Exposure of C6 glioma cells to PTX (100 ng/ml), which selectively uncouples $G_{i/o}$ from receptors, caused an almost complete suppression of ERK1/2 phosphorylation induced by amitriptyline (20 μM), imipramine (20 μM), desipramine (20 μM), nortriptyline (20 μM), mianserin (10 μM), and mirtazapine (15 μM) (Fig. 6A-C). PTX blocked LPA (100 nM)-induced stimulation of ERK1/2 phosphorylation (Fig. 6D), but failed to affect the stimulatory effect elicited by either FGF-2 (10 ng/ml) or 5-HT (10 μM) (Fig. 6D, E). Exposure to PTX also prevented ERK1/2 phosphorylation induced by either mianserin (5 μM) or amitriptyline (15 μM) in rat cortical astrocytes (Fig. 6F).

Antidepressant-induced ERK1/2 phosphorylation involves PDGF-R and FGF-R transactivation

Like other GPCRs, LPA receptors have been shown to stimulate ERK1/2 via transactivation of growth factor receptor tyrosine kinases, particularly EGF receptor (EGF-R) (Wetzker and Bohmer, 2003). Exposure of C6 glioma cells to 50 ng/ml of EGF for 5 min failed to affect ERK1/2 phosphorylation (results not shown), indicating the absence of functional EGF-R coupled to ERK1/2. On the other hand, in these cells FGF-R has been identified as a site of convergence between growth factor and $G_{i/o}$-coupled receptor signalling (Belcheva et al., 2002). We found that ERK1/2 phosphorylation elicited by either LPA, amitriptyline or mianserin was significantly reduced by pre-treatment of C6 glioma cells with the FGF-R tyrosine kinase inhibitor PD173074 at a concentration (100 nM) that completely blocked the stimulatory

JPET Fast Forward. Published on September 7, 2016 as DOI: 10.1124/jpet.116.236455
This article has not been copyedited and formatted. The final version may differ from this version.

response to FGF-2 (10 ng/ml) (Fig. 7A,B). Exposure to PD173074 (100 nM) completely blocked ERK1/2 phosphorylation induced by amitriptyline and mianserin in rat cortical astrocytes (Fig. 7C).

Acute treatment of C6 glioma cells with amitriptyline (15 µM) and mianserin (5 µM) elicited a significant increase in FGF-R phosphorylation at Tyr653/654 (Fig. 7D,E), which is critical for the receptor kinase activity and signalling (Mohammadi et al., 1996). Pre-treatment with either AM966 or Ki16425 blocked antidepressant-induced FGF-R phosphorylation (Fig. 7D,E).

In addition to FGF-2, PDGF has been shown to act on C6 glioma cells (Zhang et al., 1992; Goya et al., 1996). As shown in Fig. 7F, PDGF-BB (10 ng/ml) induced a marked autophosphorylation of PDGF-R β at Tyr751, which is located in the kinase insert region of the receptor and acts as a docking site for phosphatidylinositol 3-kinase (PI3K) (Panayotou et al., 1992). Like PDGF-BB, LPA (100 nM), clomipramine (10 µM), mianserin (5 µM) and amitriptyline (15 µM) induced a significant increase in PDGF-R β phosphorylation, although by an extent smaller than that elicited by PDGF-BB (Fig. 7G). Cell treatment with the PDGF-R tyrosine kinase inhibitor tyrphostin AG1296 (10 µM) abrogated ERK1/2 phosphorylation induced by PDGF-BB (3 ng /ml), but had no effect of the stimulation induced by FGF-2 (3 ng/ml), indicating that the inhibitor displayed receptor-specificity (Fig. 7H). Pre-treatment with tyrphostin AG1296 (10 µM) reduced ERK1/2 phosphorylation induced by either amitriptyline or mianserin (Fig. 7I).

Stimulation of Akt signalling by antidepressants through LPA_1 and growth factor receptor activity

JPET Fast Forward. Published on September 7, 2016 as DOI: 10.1124/jpet.116.236455
This article has not been copyedited and formatted. The final version may differ from this version.

Activation of the PI3K/Akt pathway is a main mechanism by which growth factor receptors induce pro-survival signalling (Hennessy et al., 2005). Plasma membrane 3'-phosphoinositides generated by PI3K allow the recruitment and the activation of Akt through phosphorylation at Thr308 by phosphatidylinositol-dependent protein kinase 1. As shown in Fig. 8A, in C6 glioma cells LPA (1μM), mirtazapine (15 μM), imipramine (10 μM), mianserin (5 μM) and amitriptyline (15 μM) caused a significant increase of Akt phosphorylation at Thr308. Cell pre-treatment with either AG1296 (10 μM) or PD173074 (100 nM) inhibited amitriptyline and mianserin-stimulated Akt phosphorylation (Fig. 8B,C). Pre-treatment with AM966 (100 nM) completely blocked the stimulation of Akt phosphorylation elicited by either amitriptyline or mianserin (Fig. 8D). Moreover, AM966 prevented the antidepressant-induced phosphorylation of GSK-3β at Ser9, a main downstream target of Akt (Hennessy et al., 2005) (Fig. 8E).

Mianserin protects glial cells from oxidative stress-induced apoptosis through LPA_1

Exposure of primary astrocytes to hydrogen peroxide (H_2O_2) has been reported to cause apoptotic cell death (Juknat et al., 2005). Immunofluorescence analysis showed that 24 h incubation of C6 glioma cells and rat cortical astrocytes with 300 and 100 μM H_2O_2, respectively, enhanced the percentage of cells positive for cleaved active form of caspase 3, a marker of apoptosis (Fig. 9A, B). The deleterious effects of H_2O_2 were markedly reduced in cells pre-treated for 24 h with mianserin (5 μM). Western blot analysis of C6 glioma cell extracts indicated that prolonged exposure to 300 μM H_2O_2 caused a significant increase in the levels of cleaved PARP, a substrate of activated caspase 3, and this effect was significantly reduced in cells

pre-treated with mianserin (5 μM) (Fig 9C). The addition of AM966 (100 nM) failed to affect H_2O_2-induced stimulation of PARP cleavage, but completely prevented the inhibitory effect of mianserin. Similarly, analysis of C6 glioma cell viability showed that mianserin (5 μM) reduced the cell death induced by H_2O_2 and that the protective effect of mianserin was attenuated in cells co-treated with AM966 (100 nM) (Fig 9D). In cortical astrocyte prolonged exposure to H_2O_2 (100 μM) enhanced the number of cell nuclei displaying DNA fragmentation, as assessed by the TUNEL assay (Fig. 9E). Pre-treatment with mianserin (5 μM) reduced this apoptotic marker to control levels and this effect was prevented by AM966 (100 nM). Exposure to H_2O_2 (200 μM) reduced astrocyte viability by 40 % ($p < 0.001$) and this effect was attenuated by pre-treatment with mianserin (5 μM) (Fig 9F). This protective effect was significantly reduced by AM966 (100 nM).

Discussion

A large number of studies have demonstrated that antidepressants affect intracellular signalling and biological activity of glial cells, but the molecular mechanisms mediating these effects are still not completely understood. In the present study we provide the first evidence that in C6 glioma cells and rat cortical astrocytes activation of $G_{i/o}$-coupled LPA_1 is involved in the stimulation of ERK1/2 signalling by tricyclic and tetracyclic antidepressants. Moreover, the study shows that mianserin inhibits oxidative stress-induced apoptosis of glial cells and that this protective effect involves LPA_1 activation.

In C6 glioma cells amitriptyline and mianserin induced a rapid and persistent increase of ERK1/2 phosphorylation with a kinetic profile similar to that displayed by

LPA. Analysis of concentration-response curves showed that LPA stimulated ERK1/2 phosphorylation with an EC_{50} of 260 nM, which agrees with the potency previously observed in CHO-K1 cells expressing endogenous LPA_1 (81 nM) and HEK 293 cells transfected with human LPA_1 cDNA (140 nM) (Olianas et al., 2015). Amitriptyline and mianserin were less potent and efficacious than LPA in stimulating ERK1/2 phosphorylation, suggesting that they behaved as partial agonists. It is noteworthy that their EC_{50} values (2.1 and 1.2 μM, respectively) are within the concentration range reached by these drugs in the brain following therapeutic doses (Glotzbach and Preskorn, 1982; Kurata and Kurachi, 1989).

ERK1/2 phosphorylation elicited by either amitriptyline or mianserin was antagonized with nanomolar potencies by structurally different LPA_1 antagonists, including AM966, which selectively inhibits LPA_1 over $LPA_{2\text{-}5}$ (Swaney et al., 2010) and Ki16425, which blocks LPA_1 and LPA_3 and has no activity at the other LPA receptors (Ohta et al., 2003; Yanagida et al., 2009; Jiang et al., 2013). VPC12249 (S), a LPA analog that is a dual LPA_1/LPA_3 antagonist (Heise et. al., 2001), was also effective in antagonizing ERK1/2 phosphorylation induced by the two antidepressants. Conversely, in C6 glioma cells the compound H2L5186303, which blocks LPA_2 about 3,000 and 100 times more potently than LPA_1 and LPA_3, respectively (Fells et al., 2008), had no effect on ERK1/2 phosphorylation elicited by either amitriptyline, mianserin or LPA over a wide concentration range. Moreover, in these cells depletion of LPA_1 by siRNA treatment led to a significant reduction of antidepressant- and LPA-induced ERK1/2 activation. Collectively, these data indicate that activation of LPA_1 plays a major role in ERK1/2 activation by amitriptyline and mianserin in both C6 glioma cells and rat cortical astrocytes.

It is important to note that, in addition to LPA_1, Western blot analysis detected the presence of LPA_2 and LPA_3, which display high sequence homology to LPA_1 (Yung et al., 2015), in both whole cell lysates and crude plasma membrane preparations of C6 glioma cells. The finding that LPA stimulated ERK1/2 exclusively via LPA_1 suggests the possibility, which remains to be investigated, that in these cells LPA_2 and LPA_3 are coupled to ERK1/2 less efficiently than LPA_1. With regard to the stimulatory effects of amitriptyline and mianserin, the selective involvement of LPA_1 is consistent with previous observations that in assays of receptor-β-arrestin interaction both antidepressants failed to show agonist activity in CHO-K1 cells over-expressing either LPA_2 or LPA_3 (Olianas et al., 2015).

The present study also provides evidence that in C6 glioma cells and primary astrocytes LPA_1 mediates antidepressant-induced signalling events occurring downstream of ERK1/2. Cell treatment with either AM966 or Ki16425 prevented the stimulation of CREB and Elk-1 phosphorylation elicited by amitriptyline and mianserin. Transcriptional activation of CREB via phosphorylation at Ser133 is known to trigger the expression of a large array of genes regulating neuronal development, synaptic plasticity, learning and memory (Lonze and Ginty, 2002). In glial cells, CREB activation has been linked not only to the expression of growth factors, but also to cell differentiation, proliferation and survival (Sato-Bigbee et al., 1999; Kim et al., 2007; Daniel et al., 2014; Pardo et al., 2016). Elk-1 is a transcription factor that upon phosphorylation by ERK1/2 translocates to the nucleus where it regulates immediate early gene expression, neuronal differentiation and cytoskeleton dynamics by binding to the serum response element (Besnard et al., 2011). There is evidence that, like CREB, Elk-1 activation induces growth factor expression and anti-

JPET Fast Forward. Published on September 7, 2016 as DOI: 10.1124/jpet.116.236455
This article has not been copyedited and formatted. The final version may differ from this version.

apoptotic effects (Demir et al., 2011; Shin et al., 2009). Thus, the present study suggests that LPA_1 may play a role in mediating antidepressant-induced pro-survival signalling via CREB and Elk-1 activation.

In agreement with our previous studies (Olianas et al., 2012), in C6 glioma cells and primary astrocytes ERK1/2 stimulation elicited by mianserin and other antidepressants, including amitriptyline, imipramine, desipramine, and mirtazapine, was suppressed by cell treatment with PTX, implying the involvement of $G_{i/o}$ family of G proteins. This finding is also consistent with the observation that in different cell types LPA_1 induces ERK1/2 activity in a PTX-sensitive manner (Ishii et al., 2004) and further supports the participation of $G_{i/o}$-coupled LPA_1 in the antidepressant actions in glial cells. PTX treatment failed to prevent ERK1/2 phosphorylation by FGF-2, indicating that this response was independent of $G_{i/o}$ activation. Moreover, under similar experimental conditions, treatment of C6 glioma cells with PTX did not prevent the stimulation of ERK1/2 phosphorylation by 5HT. While this observation is in line with the finding that astrocytes express $5HT_2$ receptors coupled to ERK1/2 via PTX-insensitive G proteins of the $G_{q/11}$ type (Li et al., 2008), it also indicates that in C6 glioma cells 5HT receptors are unlikely to participate in ERK1/2 stimulation by the tricyclic and tetracyclic antidepressants examined.

In C6 glioma cells, the signalling cascade linking antidepressant-induced LPA_1 activation to stimulation of ERK1/2 and Akt signalling appeared to involve the transactivation of both FGF-R and PDGF-R. Thus, the phosphorylation of ERK1/2 and Akt induced by amitriptyline and mianserin was diminished by either PD173074 or tyrphostin AG1296, used at concentration that selectively inhibited the tyrosine kinase activity of FGF-R and PDGF-R, respectively. Moreover antidepressants

increased the phosphorylation of FGF-R and PDGF-R at tyrosine residues critical for the receptor kinase activity and signalling. Either AM966 or Ki16425 prevented antidepressant-induced FGF-R tyrosine phosphorylation, indicating the dependence on LPA_1 activation. In agreement with previous observations (Hisaoka et al., 2007), in primary astrocytes mianserin and amitriptyline stimulation of ERK1/2 was inhibited by PD173074, indicating the involvement of FGF-R transactivation also in this cell system.

Oxidative stress arising from an increased production of nitric oxide (NO) and reactive oxygen species (ROS), such as H_2O_2 and oxygen free radicals, is considered as a critical factor in the pathogenesis of unipolar and bipolar depression (Moylan et al., 2014). It has been postulated that depression-related pathways, including activated immune-inflammatory processes, can cause an increased formation of NO and ROS and / or impairment of antioxidant defence, which may lead to cellular damage and neurotoxicity. Although astrocytes have been shown to protect neurons from H_2O_2 toxicity (Desagher et al., 1996), there is also evidence that exposure to H_2O_2 can induce apoptosis of cultured astrocytes (Juknat et al., 2005). In the present study, we show that exposure to mianserin protected C6 glioma cells and primary astrocytes from H_2O_2-induced apoptotic cell death. The antidepressant counteracted H_2O_2-induced decrease in cell viability, activation of caspase 3 and DNA fragmentation. Mianserin also inhibited H_2O_2-induced cleavage of the DNA repairing enzyme PARP, another hallmark of the apoptotic cascade. All the protective responses elicited by mianserin in C6 glioma cells and primary astrocytes were significantly reduced by AM966, indicating the participation of LPA_1.

A growing line of evidence suggests the possible involvement of LPA_1 in the physiopathogenesis of neuropsychiatric diseases. LPA_1-null mice display marked deficit in prepulse inhibition, an index of altered sensorimotor gating process, and other phenotypic changes often associated with psychiatric diseases (Harrison et al., 2003; Roberts et al., 2005). A LPA_1-null substrain, termed Malaga LPA_1 variant, shows reduced ventricular zone, increased cortical apoptosis and neuronal loss (Estivill-Torrus et al., 2008). These mice also exhibit reduced neurogenesis in adult hippocampal dentate gyrus, alterations in the levels of neurotrophic factors, and display increased anxiety-like behaviour and spatial memory deficits (Matas-Rico et al., 2008; Santin et al., 2009). More recently, it has been reported that in mice LPA_1 is necessary for conditioned fear extinction and that its absence can enhance the risk of developing affective disorders (Pedraza et al., 2014). The observation that in glial cells amitriptyline and mianserin trigger intracellular signalling through LPA_1 indicates that this receptor system may be a critical target of the central actions of different antidepressants.

Authorship contributions:

Partecipated in research design: Onali, Olianas, Dedoni.

Conducted the experiments: Olianas, Dedoni.

Performed data analysis: Olianas, Onali.

Wrote the manuscript: Onali, Olianas.

References

Belcheva MM., Haas PD, Tan Y, Heaton VM, and Coscia CJ (2002) The fibroblast growth factor receptor is at the site of convergence between μ-opioid receptor and growth factor signaling in rat C6 glioma cells. *J Pharmacol Exp Ther* **303**: 909-918.

Besnard A, Galan-Rodriguez B, Vanhoutte, P, and Caboche J (2011) Elk-1 a transcription factor with multiple facets in the brain. *Front Neurosci* **5**: 35.

Bissell MG, Rubinstein LJ, Bignami A, and Herman MM (1974) Characterization of the rat C-6 glioma maintained in organ culture system. Production of glial fibrillary acidic protein in the absence of gliofibrillogenesis. *Brain Res* **82**: 77-89.

Czeh B, and Di Benedetto B (2013) Antidepressants act directly on astrocytes: Evidence and functional consequences. *Eur Neuropsychopharmacol* **23**: 171-185.

Daniel P, Filiz G, Brown DV, Hollande F, Gonzales M, D'Abaco G, Papalexis N, Phillips WA, Malaterre J, Ramsay RG, and Mantamadiotis T (2014) Selective CREB-dependent cyclin expression mediated by the PI3K and MAPK pathways supports glioma cell proliferation. *Oncogenesis* **3**, e108; doi: 10.1038/oncsis.2014.21.

Demir O, Aysit N, Onder Z, Turkel N, Ozturk G, Sharrocks AD, and Kurnaz IA (2011) ETS-domain transcription factor Elk-1 mediates neuronal survival: SMN as a potential target. *Biochim Biophys Acta* **1812**: 652-662.

Desagher S Glowinski J, and Premont J (1996) Astrocytes protect neurons from hydrogen peroxide toxicity. *J Neurosci* **16**: 2553-2562.

Donati RJ, and Rasenick MM (2005) Chronic antidepressant treatment prevents accumulation of Gsα in cholesterol-rich, cytoskeletal-associated plasma membrane domains (lipid rafts). *Neuropsychopharmacology* **30**: 1238-1245.

Duric V, Banasr M, Licznerski P, Schmidt HD, Stockmeier CA, Simen AA, Newton SS, and Duman, RS, (2010) A negative regulator of MAP kinase causes depressive behaviour. *Nat Med* **16**: 1328-1332.

Estivill-Torrus G, Llebrez-Zayas P, Matas-Rico E, Santin L, Pedraza C, De Diego I, Del Arco I, Fernandez-Llebrez P, Chun J, and Rodriguez De Fonseca R (2008) Absence of LPA_1 signaling results in defective cortical development. *Cerebral Cortex* **18**: 938-950.

Fatemi SH. Folsom TD, Reutiman,TJ, Pandian T, Braun NN, and Haug K (2008) Chronic psychotropic drug treatment causes differential expression of connexin 43 and GFAP in frontal cortex of rats. *Schizophr Res* **104**: 127-134.

Fells JI, Tsukahara R, Fujiwara Y, Liu J, Perygin DH, Osborne DA, Tigyi G, and Parrill AL (2008) Identification of non-lipid LPA_3 antagonists by virtual screening. *Bioorg Med Chem* **16**: 6207-6217.

Glotzbach RK, and Preskorn SH (1982) Brain concentrations of tricyclic antidepressants: single-dose kinetics and relationship to plasma concentrations in chronically dosed rats. *Psychopharmacology* **78**: 25-27.

Golan M. Schreiber G, Avissar S (2010) Antidepressants increase β-arrestin2 ubiquitination and degradation by the proteasomal pathway in C6 rat glioma cells. *J Pharmacol Exp Ther* **332**: 970-976.

Goya L, Feng P-T, Aliabadi S, and Timiras, PS (1996) Effect of growth factors on the in vitro growth and differentiation of early and late passage C6 glioma cells. *Int J Devl Neuroscience* **14**: 409-417.

Harrison SM, Reayll C, Brown G, Brown JT, Cluderay JE, Crook B, Davies CH, Dawson LA, Grau E, Heidbreder C, Hemmati P, Hervieu G, Howarth A, Hughes ZA, Hunter AJ, Latcham J, Pickering S, Pugh P, Rogers DC, Shilliam CS, and Maycox PR (2003) LPA_1 receptor-deficient mice have phenotypic changes observed in psychiatric disease. *Mol Cell Neurosci* **24**: 1170-1179.

Heise CE, Santos WL, Schreihofer AM, Heasley BH, Mukhin YV, MacDonald TL, and Lynch KR (2001) Activity of 2-substituted lysophosphatidic acid (LPA) analogs at LPA receptors: discovery of a LPA_1/LPA_3 receptor antagonist. *Mol Pharmacol* **60**: 1173-1180.

Hennessy BT, Smith DL, Ram PT, Lu Y, and Mills GB (2005) Exploiting the PI3K/Akt pathway for cancer drug discovery. *Nat Rev Drug Discov* **4**: 988-1004.

Hisaoka K, Takebayashi M, Tsuchioka M, Maeda N, Nakata Y, and Yamawaki S (2007) Antidepressants increase glial cell line-derived neurotrophic factor production through monoamine-independent activation of protein tyrosine kinase and extracellular signal-regulated kinase in glial cells. *J Pharmacol Exp Ther* **321**: 148-157.

Hisaoka K, Tsuchioka M, Yano R, Maeda N, Kajitani N, Morioka N, Nakata Y, and Takebayashi M (2011) Tricyclic antidepressant amitriptyline activates fibroblast growth factor receptor (FGFR) signaling in glial cells: Involvement in glial cell line-derived neurotrophic factor (GDNF) production. *J Biol Chem* **286**: 21118-21128.

Ishii I, Fukushima N, Ye X, Chung J (2004) Lysophospholipid receptors: signaling and biology. *Annu Rev Biochem* **73**: 321-354.

Jiang G, Inoue A, Aoki J, and Prestwich GD (2013) Phosphorothioate analogs of sn-2 radyl lysophosphatidic acid (LPA): metabolically stabilized LPA receptor agonists. *Biorg Med Chem Lett* **23**:1865-1869.

Juknat AA, del Valle Armanino Mendez A, Quaglino A, Fameli CI, Mena M, and Kotler ML (2005) Melatonin prevents hydrogen peroxide-induced Bax expression in cultured rat astrocytes. *J Pineal Res* **38**: 84-92.

Khawaja X.Z, Storm S, and Liang J-J (2004) Effects of venlafaxine on p90Rsk activity in rat C6-gliomas and brain. *Neurosci Lett* **372**: 99-103.

Kim DW, Lee JH, Park SK, Yang W-M, Jeon GS, Lee YH, Chung CK, Cho SS (2007) Astrocyte expression of phosphorylated Akt, GSK3β and CREB following an excitotoxic lesion in the mouse hippocampus. *Neurochem Res* **32**: 1460-1468.

Kurata K, and Kurachi M (1989) Heterogeneous distribution of mianserin in rat brain during chronic continuous infusion. *Pharmacology* **39**: 285-290.

Li B, Zhang S, Zhang H, Nu W, Cai L, Hertz L, and Peng L (2008) Fluoxetine-mediated $5HT_{2B}$ stimulation in astrocytes causes EGF transactivation and ERK phoshorylation. *Psychopharmacology* **201**: 443-458.

Liu Q, Li B, Zhu H.-Y, Wang Y-Q, Yu J, and Wu G-C (2009) Clomipramine treatment reversed the glial pathology in a chronic unpredictable stress-induced rat model of depression. *Eur Neuropsychopharmacol* **19**: 796-805.

Lonze BE, and Ginty DD (2002) Function and regulation of CREB family transcription factors in the nervous system. *Neuron* **35**: 605-623.

Manev R, Uz T, and Manev H (2001) Fluoxetine increases the content of neurotrophic protein S100β in the rat hippocampus. *Eur J Pharmacol* **420**: R1-R2.

Matas-Rico E, Garcia-Diaz B, Llebrez-Zayas P, Lopez-Barroso D, Santin L, Pedraza C, Smith-Fernandez A, Fernandez-Llebrez P, Tellez T, Redondo M, Chun J, Rodriguez de Fonseca F, and Estivill-Torrus G (2008) Deletion of lysophosphatidic acid receptor LPA_1 reduces neurogenesis in the mouse dentate gyrus. *Mol Cell Neurosci* **39**, 342-345.

McCarty KD, and De Vellis J (1980) Preparation of separate astroglial and oligodendroglial cell cultures from rat cerebral tissue. *J Cell Biol* **85**: 890-902.

Mercier G, Lennon AM, Renouf B, Dessouroux A, Ramauge M, Courtin F, and Pierre M (2004) MAP kinase activation by fluoxetine and its relation to gene expression in cultured rat astrocytes. J Mol Neurosci **24**: 207-216.

Mohammadi, M, Dikic I, Sorokin A, Burgess WH, Jaye M, and Schlessinger J (1996) Identification of six novel autophosphorylation sites on fibroblast growth factor receptor 1 and elucidation of their importance in receptor activation and signal transduction. *Mol Cell Biol* **16**: 977-989.

Moylan S, Berk M, Dean OM, Samuni Y, Williams LJ, O'Neil A, Hayley AC, Pasco JA, Anderson G, Jacka FN, and Maes M (2014) Oxidative & nitrosative stress in depression; why so much stress ? *Neurosci Biobehav Rev* **45**: 46-62.

Nichols NR (2003) Ndrg2, a novel gene regulated by adrenal steroids and antidepressants, is highly expressed in astrocytes. Ann NY Acad Sci **1007**: 349-356.

Ohta H, Sato K, Murata N, Damirin A, Malchinkhuu E, Kon J, Kimura T, Tobo M, Yamazaki Y, Watanabe T, Yagi M, Sato M, Suzuki R, Murooka H, Sakai T., Nishitoba T, Im D-S, Nochi H, Tamoto K, Tomura H, and Okajima F (2003) Ki16425, a subtype-selective antagonist for EDG-family lysophosphatidic acid receptors. *Mol Pharmacol* **64**: 994-1005.

Olianas MC, Dedoni S, and Onali P (2015) Antidepressants activate the lysophosphatidic acid receptor LPA_1 to induce insulin-like growth factor-I receptor transactivation, stimulation of ERK1/2 signaling and cell proliferation in CHO-K1 fibroblasts. *Biochem Pharmacol* **95**: 311-323.

Olianas MC, Dedoni S, and Onali P (2012) The atypical antidepressant mianserin exhibits agonist activity at κ-opioid receptors. *Br J Pharmacol* **167**: 1329-1341.

Olianas MC, Dedoni S, Boi M, and Onali P (2008) Activation of nociceptin/orphanin FQ-NOP receptor system inhibits tyrosine hydroxylase phosphorylation, dopamine synthesis and dopamine D1 receptor signaling in rat nucleus accumbens and dorsal striatum. *J Neurochem* **107**: 544-556.

Onali P, Dedoni S, and Olianas MC (2010) Direct agonist activity of tricyclic antidepressants at distinct opioid receptor subtypes. *J Pharmacol Exp Ther* **332**: 255-265.

Panayotou G, Bax B, Gout I, Federwisch M, Wroblowski B, Dhand R, Fry MJ, Blundell TL, Wollmer A, and Waterfield MD (1992) Interaction of the p85 subunit of PI 3-kinase and its N-terminal SH2 domain with a PDGF receptor phosphorylation site; structural features and analysis of conformational changes. *EMBO J* **11**: 4261-4272.

Pardo L, Schluter A, Valor LM, Barco A, Giralt M, Golbano A, Hidalgo J, Jia P, Zhao Z, Jove' M, Portero-Otin M, Ruiz M, Gimenez-Llort L, Masgrau R, Pujol A, and Galea E (2016) Targeted activation of CREB in reactive astrocytes is neuroprotective in focal acute cortical injury. *Glia* **64**: 853-874.

Pedraza C, Lopez-Sanchez J, Castilla-Ortega E, Rosell-Valle C, Zambrana-Infantes E, Garcia-Fernandez M, Rodriguez de Fonseca F, Chun J, Santin LJ, and Estivill-Torrus G (2014) Fear extinction and acute stress reactivity reveal a role of LPA1 receptor in regulating emoziona-like behaviors. *Brain Struct Funct* **219**: 1659-1672.

Pfeiffer SE, Herschman HR, Lightbody J, and Sato G (1970). Synthesis by a clonal line of rat glial cells of a protein unique to the nervous system. *J Cell Physiol* **75**: 329-340.

Raff MC, Abnev ER, Cohen J, Lindsay R, and Noble M (1983) Two types of astrocytes in cultures of developing rat white matter: differences in morphology, surface gangliosides, and growth characteristics. *J Neurosci* **3**: 1289-1300.

Ramakers GJA, and Moolenaar WH (1998) Regulation of astrocyte morphology by RhoA and lysophosphatidic acid. *Exp Cell Res* **245**: 252-262.

Reagan LP, Rosell DR, Wood GE, Spedding M, Munoz C, Rothstein J, and McEwen BS (2004) Chronic restraint stress up-regulates GLT-1 mRNA and protein expression in the rat hippocampus: reversal by tianeptine. *Proc Natl Acad Sci USA* **101**: 2179-2184.

Roberts C, Winter P, Shilliam CS, Hughes ZA, Langmead C, Maycox PR, and Dawson LA (2005) Neurochemical changes in LPA_1 receptor deficient mice – A putative model of schizophrenia. *Neurochem Res* **30**: 371-377.

Roux PP, and Blenis J (2004) ERK and p38 MAPK-activated protein kinase: a family of protein kinases with diverse biological functions. *Microbiol Mol Biol Rev* **68**: 320-344.

Sanacora G, and Banasr M (2013) From pathophysiology to novel antidepressant drugs: glial contributions to the pathology and treatment of mood disorders. *Biol Psychiatry* **73**: 1172-1179.

Santin LJ, Bilbao A, Pedraza C, Matas-Rico E. Lopez-Barroso D, Castilla-Ortega E, Sanchez-Lopez J, Riquelme R, Varela-Nieto I, de la Villa P, Suardiaz M, Chun J, Rodriguez De Fonseca F, and Estivill-Torrus G (2009) Behavioral phenotype of

maLPA$_1$-null mice: increased anxiety-like behavior and spatial memory deficits. *Genes Brain Behav* **8**: 772-784.

Sato K, Horiuchi Y, Jin Y, Malchinkhuu E, Komachi M, Kondo T, and Okajima F (2011) Unmasking of LPA$_1$ receptor-mediated migration response to lysophosphatidic acid by interleukin-1β-induced attenuation of Rho signaling pathways in rat astrocytes. *J Neurochem* **117**:164-174.

Sato-Bigbee C, Pal S, and Chu AK (1999) Different neuroligands and signal transduction pathways stimulate CREB phosphorylation at specific developmental stages along oligodendrocyte differentiation. *J Neurochem* **72**: 139-147.

Shin SY, Song H, Kim CG, Choi Y-K, Lee KS, Lee S-J, Lee H-J., Lim Y, and Lee YH (2009) Egr-1 is necessary for fibroblast growth factor-2-induced transcriptional activation of the glial cell line-derived neurotrophic factor in murine astrocytes. *J Biol Chem* **284**: 30583-30593.

Sillaber I, Panhuysen M, Henninger MSH, Ohl F, Kuhne C, Putz B, Pohl T, Deussing JM, Paez-Pereda M, and Holsboer F (2008) Profiling of behavioural changes and hippocampal gene expression in mice chronically treated with the SSRI paroxetine. *Psychopharmacology* **200**: 557-572.

Spohr TC, Choi JW, Gardell SE, Herr DR, Kastrup Rehen S, Carvalho Alcantara Gomes F, Chun J (2008) Lysophosphstidic acid receptor-dependent secondary effects via astrocytes promote neuronal differentiation. J Biol Chem **283**: 7470-7479.

Swaney JS, Chapman C, Correa LD, Stebbins KJ, Bundey RA, Prodanovich PC, Fagan P, Baccei CS, Santini AM, Hutchinson JH, Seiders TJ, Parr TA, Prasit P, Evans JF, and Lorrain DS (2010) A novel, orally active LPA_1 receptor antagonist inhibits lung fibrosis in the mouse bleomycin model. *Br J Pharmacol* **160**:1699-1713.

Tabuchi S, Kume K, Aihara M, and Shimizu T (2000) Expression of lysophosphatidic acid receptor in rat astrocytes: mitogenic effect and expression of neurotrophic genes. *Neurochem Res* **25**: 573-582.

Wetzker R, and Bohmer F-D (2003) Transactivation joins multiple tracks to the ERK/MAPK cascade. *Nat Rev* **4**: 651-657.

Yanagida K, Masago K, Nakanishi H, Kihara Y., Hamano F, Tajima Y, Taguchi R, Shimizu T, and Ishii S (2009) Identification and characterization of a novel lysophosphatidic acid receptor, p2y5/LPA6. *J Biol Chem* **284**: 17731-17741.

Yung YC, Stoddard NC, Mirendil H, and Chun J (2015) Lysophosphatidic acid signaling in the nervous system. *Neuron* **85**: 669-682.

Zhang W, Nakashima T, Sakai N, Yamada H, Okano Y, Nozawa Y (1992) Activation of phospholipase D by platelet-derived growth factor (PDGF) in rat C6 glioma cells: possible role in mitogenic signal transduction. *Neurol Res* **14**: 397-401.

*This work was supported by Regione Autonoma della Sardegna, Italy, L.R. n.7/2007 [CRP10810/2012] and Fondazione Banco di Sardegna, Italy [Prot. U993.2014/AI.875.MGB] to P.O.

Figure legends

Fig. 1. Time- and concentration-dependent stimulation of ERK1/2 phosphorylation by amitriptyline, mianserin and LPA in C6 glioma cells. Cells were serum starved for 24 h and then exposed to either amitriptyline (15 µM) (A) mianserin (5 µM) (B) or LPA (100 nM) (C) for the indicated periods of time. The levels of phospho-ERK1/2 and total ERK1/2 were measured in cell extracts by Western blot. Densitometric ratios are expressed as fold of stimulation with respect to 0 time (vehicle-treated cells) and are the mean ± SEM of four experiments. * $P < 0.05$, *** $P < 0.001$ vs 0 time by ANOVA followed by Newman-Keuls *post hoc* test. (D-F) Serum-starved cells were treated for 10 min with the indicated concentrations of amitriptyline, mianserin and LPA. Values are expressed as fold of stimulation with respect to control (vehicle-treated cells) and are the mean ± SEM of five experiments.

Fig. 2. Blockade of antidepressant- and LPA-induced ERK1/2 phosphorylation by LPA receptor antagonists. (A) C6 glioma cells were pre-incubated for 10 min with either vehicle, AM966 (1 µM) (AM) or Ki16425 (1 µM) (Ki) and then exposed to either vehicle or LPA (100 nM) for 10 min. Values are expressed as fold of stimulation with respect to control (vehicle+ vehicle) and are the mean ± SEM of three experiments. (B) C6 glioma cells were pre-incubated for 10 min with either vehicle, Ki16425 (100 nM) or AM966 (100 nM) and then exposed to either vehicle or amitriptyline (15 µM) (Amitript) for 10 min. Values are the mean ± SEM of five experiments. (C) C6 glioma cells were pre-incubated as indicated in (B) and then exposed to either vehicle or mianserin (5 µM) (Mians) for 10 min. Values are the mean ± SEM of five experiments. (D) C6 glioma cells were pre-incubated for 10 min with either vehicle or

10 µM VPC12249 (S) and then exposed to either vehicle, 15 µM amitriptyline or 5 µM mianserin for 10 min. Values are the mean ± SEM of three experiments. (E) Astrocytes were pre-incubated with the LPA receptor antagonists as indicated in (A) and then exposed to either vehicle or 1 µM LPA for 15 min. Values are the mean ± SEM of five experiments. (F-H) Astrocytes were pre-incubated for 10 min with either vehicle, 100 nM Ki16425, 100 nM AM966 or 10 µM VPC12249 and then exposed to either vehicle, 15 µM amitriptyline or 5 µM mianserin for 15 min. Values are the mean ± SEM of four experiments. *** $P < 0.001$ vs control (vehicle + vehicle); $^{\#}$ $P < 0.05$, $^{\#\#}$ $P < 0.01$, $^{\#\#\#}$ $P < 0.001$ vs the corresponding sample treated with vehicle by ANOVA followed by Newman-Keuls *post hoc* test.

Fig. 3. Concentration-dependent effects of LPA receptor antagonists on antidepressant- and LPA-induced ERK1/2 phosphorylation in C6 glioma cells. Cells were pre-incubated with either vehicle or the indicated concentrations of AM966 or Ki16425 for 10 min and then exposed to either vehicle or 1 µM LPA (A, B), 15 µM amitriptyline (C, D) or 5 µM mianserin (E, F) for 10 min. Values are expressed as percent of phospho-ERK1/2 stimulation and are the mean ± SEM of four separate experiments. (G) Cells were pre-incubated for 10 min with either vehicle or the indicated concentrations of H2L5186303 (H2L5) and then exposed to either vehicle or 1 µM LPA for 10 min. Values are the mean ± SEM of three experiments. (H) Cells were pre-incubated with either vehicle or 1 µM H2L5186303 (H2L5) and then exposed to either vehicle, 15 µM amitriptyline or 5 µM mianserin for 10 min. Values are the mean ± SEM of three experiments. *** $P < 0.001$ vs control (vehicle+vehicle).

Fig. 4. LPA_1 knockdown attenuates antidepressant- and LPA-induced ERK1/2 phosphorylation in C6 glioma cells. (A) Whole cell lysates and crude plasma membranes were analyzed for LPA_1, LPA_2 and LPA_3 expression by Western blot. GAPDH and pan-cadherin (plasma membrane marker) were used as loading controls. Data are representative of three separate experiments. (B) Cells were treated with either control siRNA or LPA_1 siRNA and were analyzed for LPA_1, LPA_2 and LPA_3 expression 48 h post-transfection. Each lane was loaded with a sample from three separate transfections. Values of LPA_{1-3} immunoreactivities normalized to the levels of GAPDH are reported as percent of control (control siRNA-treated cells) and are the mean ± SEM of three experiments. (C, D) C6 glioma cells treated with siRNAs as indicated in (B) were exposed for 10 min to either vehicle, amitriptyline (15 µM), mianserin (5 µM) (C), imipramine (15 µM) or LPA (50 nM) (D). Values are the mean ± SEM of three experiments. *** $P < 0.001$ vs control, $^{\#}$ $P < 0.05$, $^{\#\#\#}$ $P < 0.001$ vs the corresponding sample in control siRNA-treated group by ANOVA followed by Newman-Keuls *post hoc* test.

Fig. 5. Blockade of LPA_1 prevents the phosphorylation of CREB and ElK-1 induced by amitriptyline and mianserin. (A) C6 glioma cells were serum-starved for 24 h, pre-treated with either vehicle or 100 nM Ki16425 for 10 min and then exposed to either vehicle or 15 µM amitriptyline for 30 min. Phospho-CREB immunofluorescence (green color) was measured in nuclei identified by DAPI staining (blue color). Bar = 50 µm. Values of quantitative analysis of phospho-CREB immunofluorescence are expressed as percent of positive nuclei and are the mean ± SEM of three experiments. *** $P < 0.001$ vs control; $^{\#\#\#}$ $P < 0.001$ vs the respective value with no

antagonist by ANOVA followed by Newman-Keuls *post hoc* test. C6 glioma cells (B) and rat astrocytes (C) were pre-incubated with either vehicle or AM966 (100 nM) for 10 min and then exposed for 30 min to either 15 µM amitriptyline or 5 µM mianserin. Cell extracts were then analyzed for phospho-CREB (pCREB) and total CREB by Western blot. Values are the mean ± SEM of four experiments. (D) C6 glioma cells were treated as indicated in (B) and cell extracts were analyzed for phospho-Elk-1 (pElk-1) and total Elk-1. Values are the mean ± SEM of three experiments. ** $P < 0.01$, *** $P < 0.001$ vs control; $^{\#}$ $P < 0.05$, $^{\#\#\#}$ $P < 0.001$ by ANOVA followed by Newman-Keuls *post hoc* test.

Fig. 6. PTX-sensitive G proteins transduce antidepressant-induced ERK1/2 phosphorylation. C6 glioma cells were incubated in serum-free medium containing either vehicle or 100 ng/ml of PTX for 24 h and then treated for 10 min with either vehicle, 20 µM amitriptyline, 20 µM imipramine (Imipr) (A), 20 µM desipramine (Desipr), 20 µM nortriptyline (Nortript) (B), 10 µM mianserin or 15 µM mirtazapine (Mirtaz) (C). In (D) vehicle- and PTX-treated cells were exposed for 10 min to either 100 nM LPA or 10 ng/ml FGF-2. Values are the mean ± SEM of four experiments. (E) Serum-starved C6 glioma cells pre-incubated with either vehicle or PTX as indicated in (A) were exposed for 10 min to 5 µM mianserin and for 5 min to 10 µM 5HT. Values are the mean ± SEM of three experiments. (F) Rat cortical astrocytes were pre-incubated with either vehicle or PTX as indicated in (A) and then exposed to 5 µM mianserin or 15 µM amitriptyline for 15 min. Values are the mean ± SEM of four experiments. *** $P < 0.001$ vs control (vehicle); $^{\#\#\#}$ $P < 0.001$ by ANOVA followed by Newman-Keuls *post hoc* test.

Fig. 7. Involvement of growth factor receptor transactivation in antidepressant- and LPA-induced ERK1/2 phosphorylation. (A, B) Serum-starved C6 glioma cells were pre-treated with either vehicle or the FGF-R inhibitor PD173074 (100 nM) for 2 h and then exposed for 10 min to 15 µM amitriptyline, 10 ng/ml FGF-2, 5 µM mianserin or 50 nM LPA. Values are the mean ± SEM of four experiments. (C) Rat cortical astrocytes were pre-treated with either vehicle or PD173074 as indicated in (A) and then exposed for 15 min to either 15 µM amitriptyline or 5 µM mianserin. Values are the mean ± SEM of four experiments. *** $P < 0.001$ vs control; $^{\#}P < 0.05$, $^{\#\#\#}P < 0.001$ vs the corresponding value in vehicle pre-treated group by ANOVA followed by Newman-Keuls *post hoc* test. (D, E) C6 glioma cells were pre-incubated with either vehicle, 100 nM AM966 or 100 nM Ki16425 for 10 min and then exposed for 5 min to either 15 µM amitriptyline or 5 µM mianserin, respectively. Cell extracts were analyzed for the levels of phospho-Tyr653/654-FGF-R (p-FGF-R) and total FGF-R. Values are the mean ± SEM of four experiments. *** $P < 0.001$ vs control; $^{\#\#}P < 0.01$, $^{\#\#\#}P < 0.001$ by ANOVA followed by Newman-Keuls *post hoc* test. C6 glioma cells were treated for 5 min with either vehicle and 10 ng/ml PDGF-BB (F), or vehicle, 100 nM LPA, 10 µM clomipramine (Clomipr), 5 µM mianserin, and 15 µM amitriptyline (G). Cell extracts were analyzed for the levels of phospho-Tyr751-PDGF-R β (p-PDGF-R) and total PDGF-R β (PDGF-R) by Western blot. Values are the mean ± SEM of four experiments. (H, I) C6 glioma cells were pre-incubated for 1 h with either vehicle or 10 µM tyrphostin AG1296 (AG1296) and then exposed for 10 min to either 3 ng/ml PDGF-BB, 3 ng/ml FGF-2, 15 µM amitriptyline or 5 µM mianserin. Values are the mean ± SEM of four experiments. * $P < 0.05$, *** $P < 0.001$

JPET Fast Forward. Published on September 7, 2016 as DOI: 10.1124/jpet.116.236455
This article has not been copyedited and formatted. The final version may differ from this version.

vs control, ### $P < 0.001$ vs the corresponding value in vehicle-treated group by either ANOVA followed by Newman-Keuls *post hoc* test (G, I) or Student' t test (G).

Fig.8. Antidepressants induce Akt phosphorylation through LPA_1 and growth factor receptor activity. (A) C6 glioma cells were exposed for 10 min to vehicle, 1 µM LPA, 15 µM mirtazapine (Mirtaz), 10 µM imipramine (Imipr), 5 µM mianserin and 15 µM amitriptyline. Cell extracts were then analyzed for phospho-Thr308-Akt (pAkt) and total Akt by Western blot. Values are the mean ± SEM of four experiments. (B, C) C6 glioma cells were pre-treated with either vehicle and 10 µM tyrphostin AG1296 for 1 h (B), or vehicle and 100 nM PD173074 for 2 h (C). Thereafter, cells were exposed for 10 min to either vehicle, 15 µM amitriptyline or 5 µM mianserin. Values are the mean ± SEM of four experiments. (D, E) C6 glioma cells were pre-incubated with either vehicle or AM966 (100 nM) for 10 min and then exposed for 10 min to either 15 µM amitriptyline or 5 µM mianserin. Cells extracts were analyzed for phospho-Akt and total Akt (D) and for phospho-Ser9-GSK-3β (pGSK3β) and total GSK-3β (E). Values are the mean ± SEM of four experiments. *** $P < 0.001$ vs control. # $P < 0.05$, ### $P < 0.001$ vs the corresponding sample treated with vehicle by ANOVA followed by Newman-Keuls *post hoc* test.

Fig.9. Mianserin protects glial cells from oxidative stress-induced apoptosis through LPA_1. C6 glioma cells (A) and rat cortical astrocytes (B) were pre-treated for 24 h in serum-free medium with either vehicle or 5 µM mianserin. Thereafter, C6 glioma cells and astrocytes were exposed for 24 h to 300 and 100 µM H_2O_2, respectively. Cells positive for cleaved caspase 3 immunofluorescence (green color) were identified and

their number expressed as percent of total cells present in each field examined. Cell nuclei are stained in blue with DAPI. Values are the mean ± SEM of four independent experiments. Bar = 50 µm (C) C6 glioma cells were pre-treated for 10 min with either vehicle or 100 nM AM966, and then exposed for 24 h in serum-free medium to either vehicle or 5 µM mianserin. Cells were then incubated in the absence and in the presence of 300 µM H_2O_2 for 24 h. Cell extracts were analyzed for cleaved PARP (cleav PARP) and PARP by Western blot. Values are the mean ± SEM of four experiments. (D) C6 glioma cells were treated as indicated in (C) and cell viability was determined by cytofluorimetric analysis using the Muse Cell Count and Viability kit. Values are expressed as percent of control (vehicle + vehicle) and are the mean ± SEM of four experiments. (E) Astrocytes were pre-treated as indicated in (B) and then incubated for 24 h with either vehicle or 100 µM H_2O_2. The number of nuclei displaying DNA fragmentation by in situ TUNEL assay (green color) was determined in each field and reported as percent of total nuclei (stained in blue with DAPI). Values are the mean ± SEM of four experiments. (F) Serum-starved rat astrocytes were pre-treated for 10 min with either vehicle or 100 nM AM966, and then exposed for 18 h to either vehicle or 5 µM mianserin. Cells were then incubated in the absence and in the presence of freshly prepared 200 µM H_2O_2 for 3 h. Cell viability was determined by the MTT assay. Values are expressed as percent of control (vehicle + vehicle) and are the mean ± SEM of four experiments. *** $P < 0.001$ vs control (vehicle); $^{\#}$ $P < 0.05$, $^{\#\#\#}$ $P < 0.001$ by ANOVA followed by Newman-Keuls *post hoc* test.

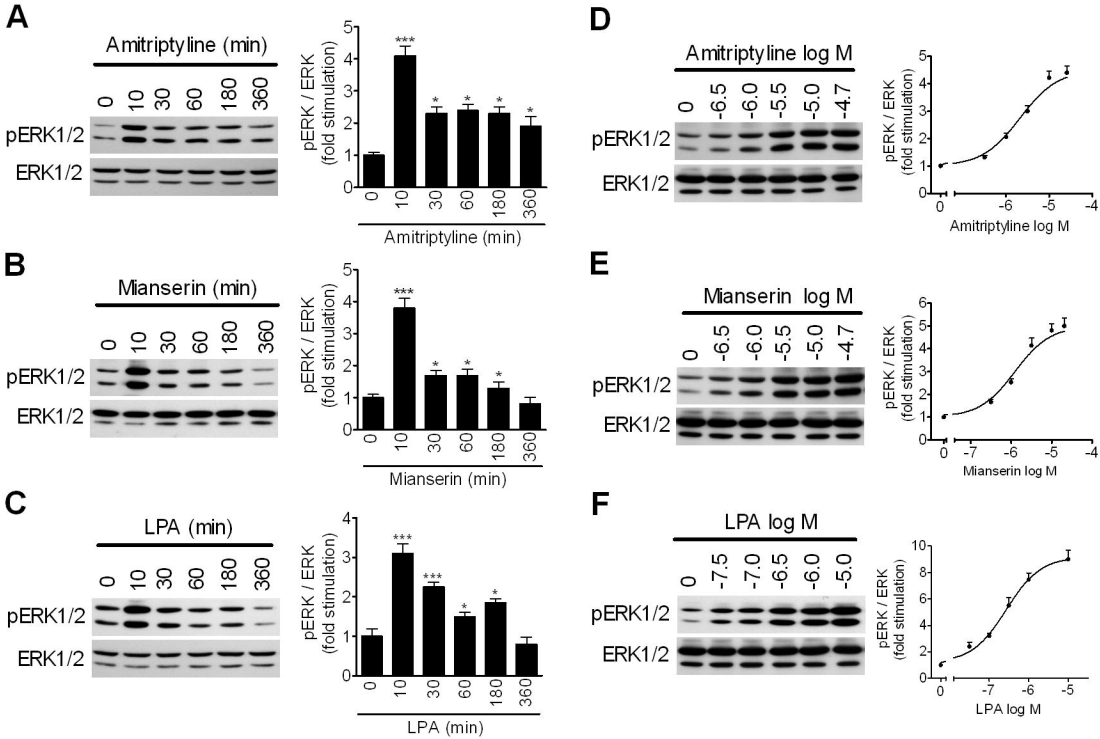
A
Amitriptyline (min)
0
10
30
60
180
360
pERK1/2
ERK1/2
pERK / ERK (fold stimulation)
Amitriptyline (min)
B
Mianserin (min)
Mianserin (min)
C
LPA (min)
LPA (min)
D
Amitriptyline log M
0
-6.5
-6.0
-5.5
-5.0
-4.7
Amitriptyline log M
E
Mianserin log M
Mianserin log M
F
LPA log M
0
-7.5
-7.0
-6.5
-6.0
-5.0
LPA log M

Fig. 1

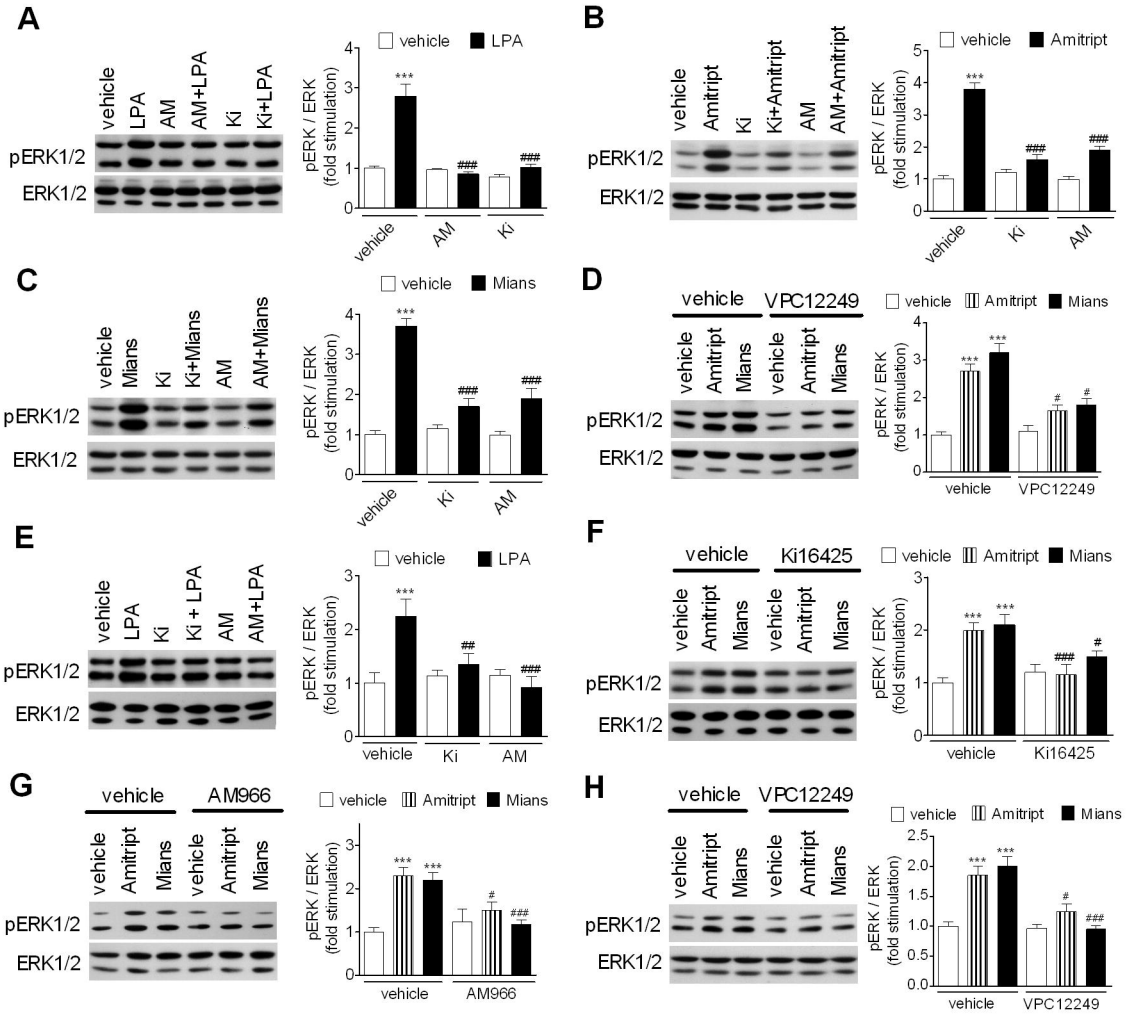
A
vehicle
LPA
AM
AM+LPA
Ki
Ki+LPA
pERK1/2
ERK1/2
pERK / ERK (fold stimulation)
vehicle
LPA
AM
Ki
B
vehicle
Amitript
Ki
Ki+Amitript
AM
AM+Amitript
Amitript
C
vehicle
Mians
Ki
Ki+Mians
AM
AM+Mians
Mians
D
VPC12249
E
vehicle
LPA
Ki
Ki + LPA
AM
AM+LPA
F
Ki16425
G
AM966
H

Fig. 2

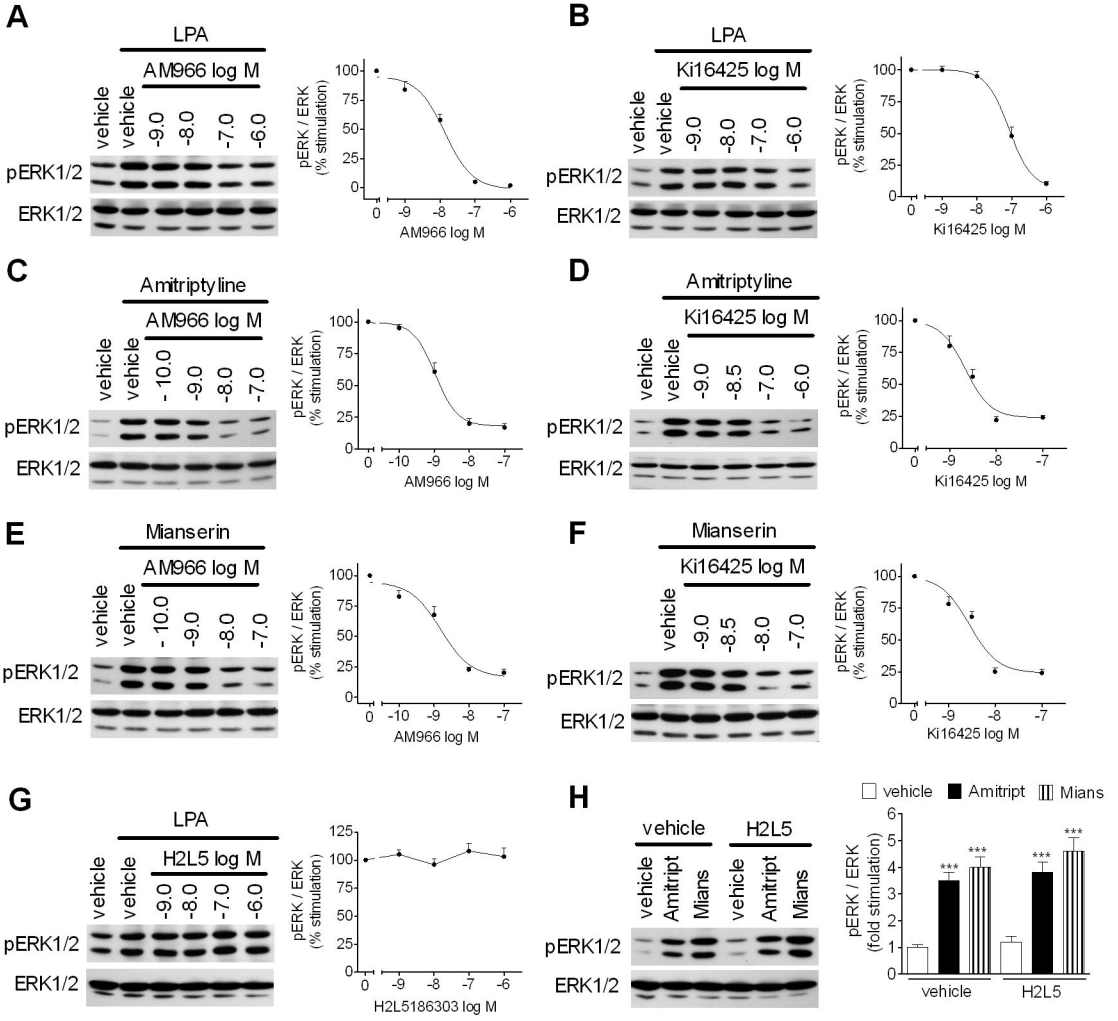
A
LPA
AM966 log M
vehicle
vehicle
-9.0
-8.0
-7.0
-6.0
pERK1/2
ERK1/2
pERK / ERK (% stimulation)
AM966 log M
B
LPA
Ki16425 log M
Ki16425 log M
C
Amitriptyline
AM966 log M
- 10.0
-9.0
-8.0
-7.0
D
Amitriptyline
Ki16425 log M
-9.0
-8.5
-7.0
-6.0
E
Mianserin
AM966 log M
F
Mianserin
Ki16425 log M
G
LPA
H2L5 log M
H2L5186303 log M
H
vehicle
H2L5
Amitript
Mians
pERK / ERK (fold stimulation)
***

Fig. 3

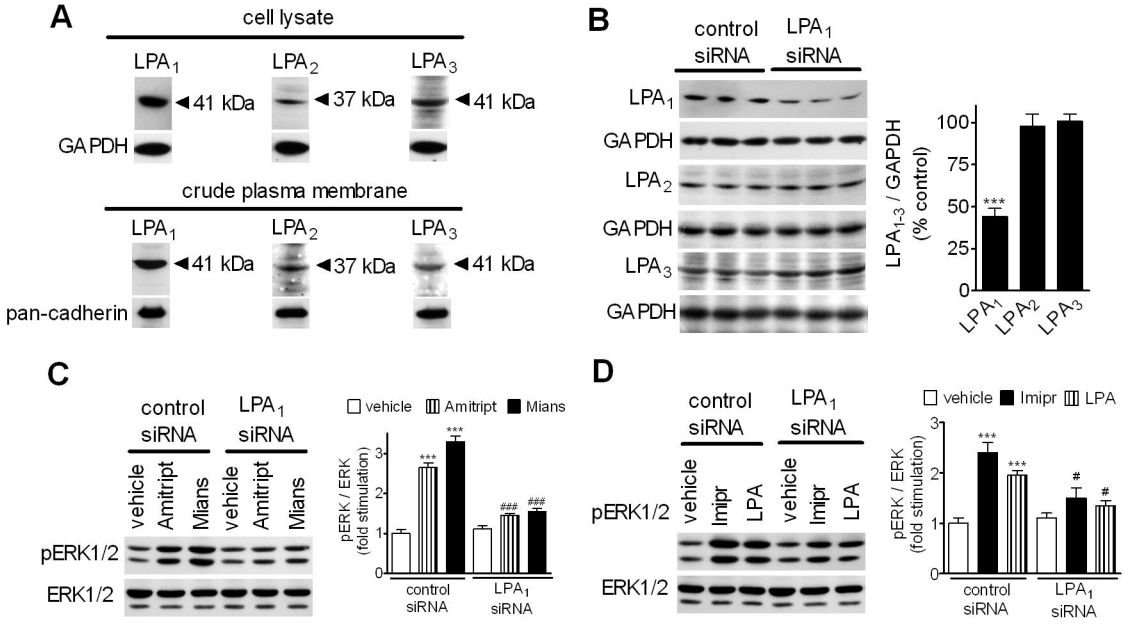
A
cell lysate
LPA1
LPA2
LPA3
41 kDa
37 kDa
41 kDa
GAPDH
crude plasma membrane
LPA1
LPA2
LPA3
41 kDa
37 kDa
41 kDa
pan-cadherin
B
control siRNA
LPA1 siRNA
LPA1
GAPDH
LPA2
GAPDH
LPA3
GAPDH
LPA1-3 / GAPDH (% control)
100
75
50
25
0
***
LPA1
LPA2
LPA3
C
control siRNA
LPA1 siRNA
vehicle
Amitript
Mians
vehicle
Amitript
Mians
pERK1/2
ERK1/2
vehicle
Amitript
Mians
pERK / ERK (fold stimulation)
***
***
###
###
control siRNA
LPA1 siRNA
D
control siRNA
LPA1 siRNA
vehicle
Imipr
LPA
vehicle
Imipr
LPA
pERK1/2
ERK1/2
vehicle
Imipr
LPA
pERK / ERK (fold stimulation)
***
***
#
#
control siRNA
LPA1 siRNA

Fig. 4

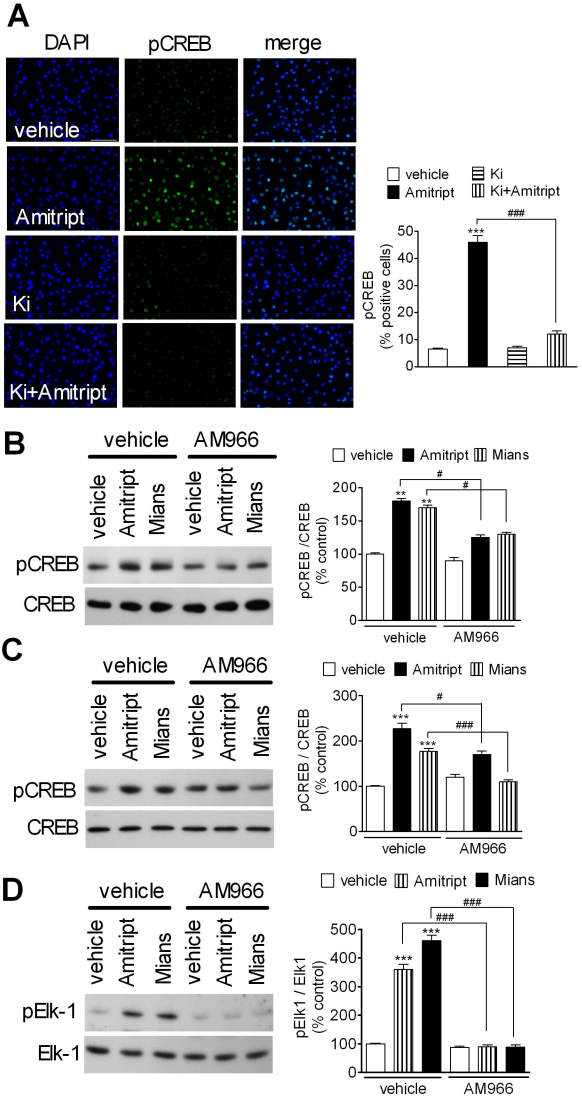
A
DAPI
pCREB
merge
vehicle
Amitript
Ki
Ki+Amitript
vehicle
Amitript
Ki
Ki+Amitript
pCREB
(% positive cells)
***
###
B
vehicle
AM966
vehicle
Amitript
Mians
vehicle
Amitript
Mians
pCREB
CREB
vehicle
Amitript
Mians
pCREB /CREB
(% control)
**
#
vehicle
AM966
C
vehicle
AM966
vehicle
Amitript
Mians
vehicle
Amitript
Mians
pCREB
CREB
vehicle
Amitript
Mians
pCREB / CREB
(% control)
***
#
###
vehicle
AM966
D
vehicle
AM966
vehicle
Amitript
Mians
vehicle
Amitript
Mians
pElk-1
Elk-1
vehicle
Amitript
Mians
pElk1 / Elk1
(% control)
***
###
vehicle
AM966

Fig. 5

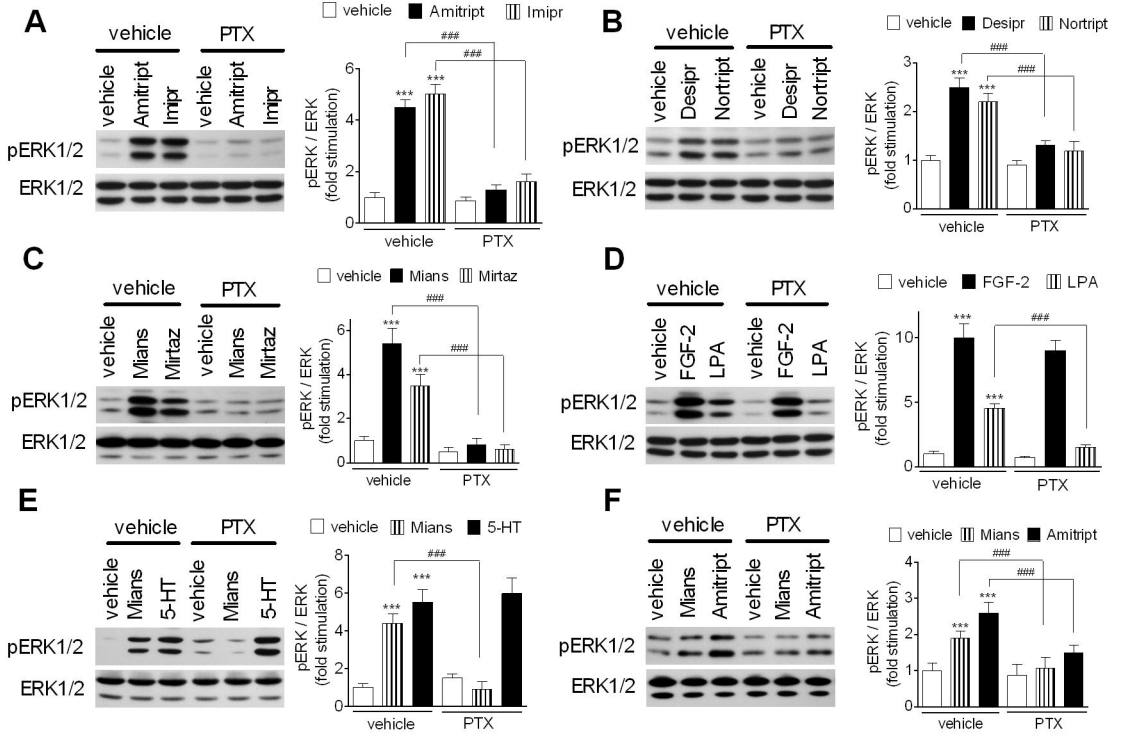
A
vehicle
PTX
vehicle
Amitript
Imipr
vehicle
Amitript
Imipr
pERK1/2
ERK1/2
vehicle
Amitript
Imipr
pERK / ERK
(fold stimulation)
###
###
***
***
vehicle
PTX
B
vehicle
PTX
vehicle
Desipr
Nortript
vehicle
Desipr
Nortript
pERK1/2
ERK1/2
vehicle
Desipr
Nortript
pERK / ERK
(fold stimulation)
###
###
***
***
vehicle
PTX
C
vehicle
PTX
vehicle
Mians
Mirtaz
vehicle
Mians
Mirtaz
pERK1/2
ERK1/2
vehicle
Mians
Mirtaz
pERK / ERK
(fold stimulation)
###
###
***
***
vehicle
PTX
D
vehicle
PTX
vehicle
FGF-2
LPA
vehicle
FGF-2
LPA
pERK1/2
ERK1/2
vehicle
FGF-2
LPA
pERK / ERK
(fold stimulation)
###
***
***
vehicle
PTX
E
vehicle
PTX
vehicle
Mians
5-HT
vehicle
Mians
5-HT
pERK1/2
ERK1/2
vehicle
Mians
5-HT
pERK / ERK
(fold stimulation)
###
***
***
vehicle
PTX
F
vehicle
PTX
vehicle
Mians
Amitript
vehicle
Mians
Amitript
pERK1/2
ERK1/2
vehicle
Mians
Amitript
pERK / ERK
(fold stimulation)
###
###
***
***
vehicle
PTX

Fig. 6

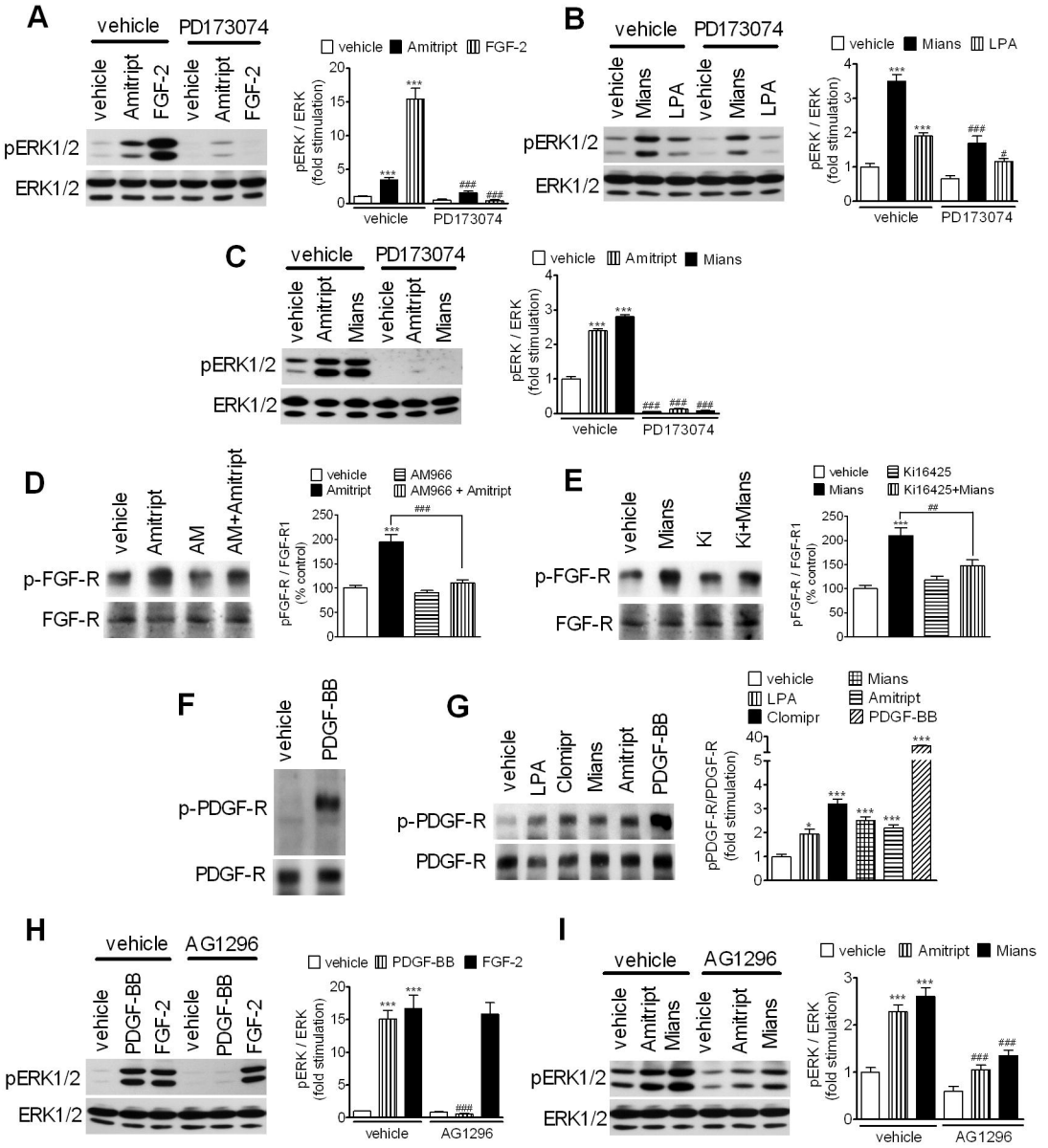
A
vehicle
PD173074
vehicle
Amitript
FGF-2
vehicle
Amitript
FGF-2
pERK1/2
ERK1/2
vehicle
Amitript
FGF-2
pERK / ERK
(fold stimulation)
vehicle
PD173074
B
vehicle
PD173074
vehicle
Mians
LPA
vehicle
Mians
LPA
pERK1/2
ERK1/2
vehicle
Mians
LPA
pERK / ERK
(fold stimulation)
vehicle
PD173074
C
vehicle
PD173074
vehicle
Amitript
Mians
vehicle
Amitript
Mians
pERK1/2
ERK1/2
vehicle
Amitript
Mians
pERK / ERK
(fold stimulation)
vehicle
PD173074
D
vehicle
Amitript
AM
AM+Amitript
p-FGF-R
FGF-R
vehicle
Amitript
AM966
AM966 + Amitript
pFGF-R / FGF-R1
(% control)
E
vehicle
Mians
Ki
Ki+Mians
p-FGF-R
FGF-R
vehicle
Mians
Ki16425
Ki16425+Mians
pFGF-R / FGF-R1
(% control)
F
vehicle
PDGF-BB
p-PDGF-R
PDGF-R
G
vehicle
LPA
Clomipr
Mians
Amitript
PDGF-BB
p-PDGF-R
PDGF-R
vehicle
LPA
Clomipr
Mians
Amitript
PDGF-BB
pPDGF-R/PDGF-R
(fold stimulation)
H
vehicle
AG1296
vehicle
PDGF-BB
FGF-2
vehicle
PDGF-BB
FGF-2
pERK1/2
ERK1/2
vehicle
PDGF-BB
FGF-2
pERK / ERK
(fold stimulation)
vehicle
AG1296
I
vehicle
AG1296
vehicle
Amitript
Mians
vehicle
Amitript
Mians
pERK1/2
ERK1/2
vehicle
Amitript
Mians
pERK / ERK
(fold stimulation)
vehicle
AG1296

Fig. 7

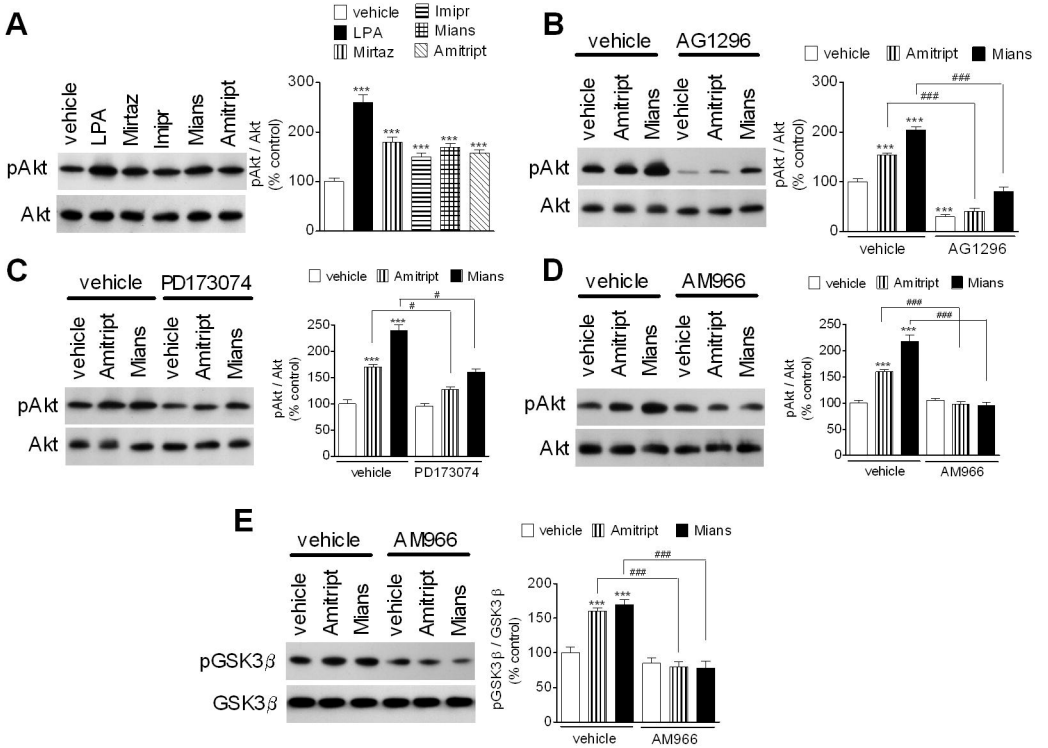
A
vehicle
LPA
Mirtaz
Imipr
Mians
Amitript
pAkt
Akt
pAkt / Akt (% control)
B
vehicle
AG1296
Amitript
Mians
C
PD173074
D
AM966
E
pGSK3β
GSK3β
pGSK3β / GSK3β (% control)

Fig. 8

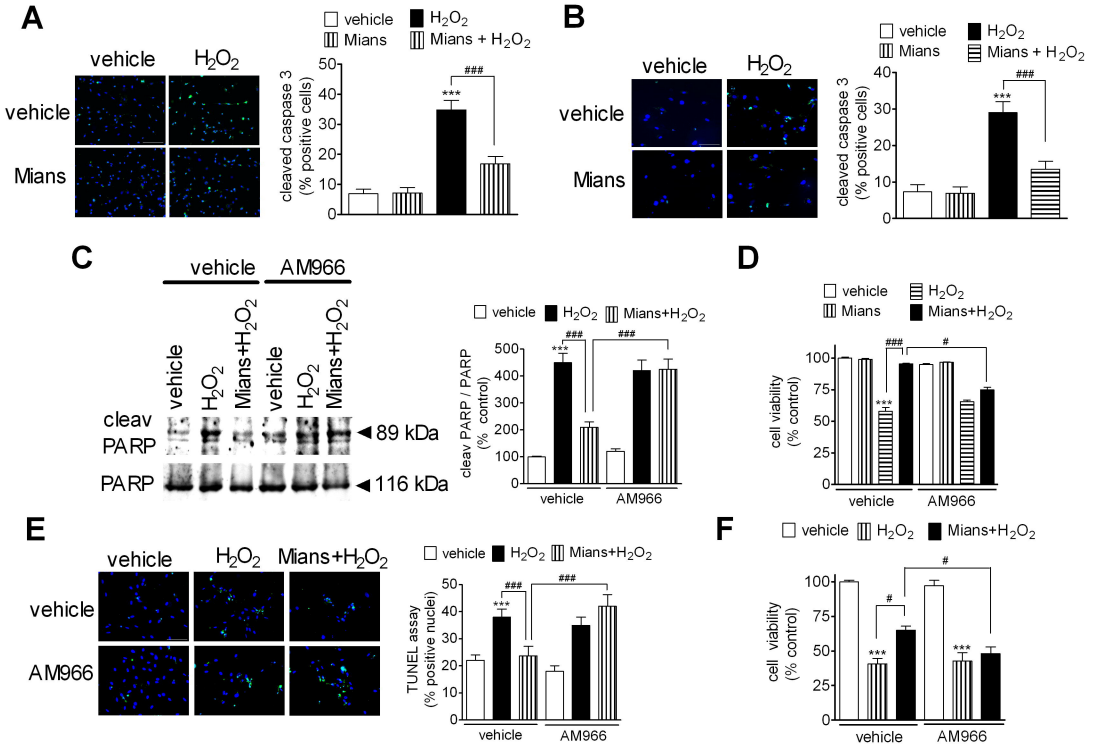
A
vehicle
H2O2
vehicle
Mians
vehicle
H2O2
Mians
Mians + H2O2
cleaved caspase 3
(% positive cells)
***
###
B
vehicle
H2O2
vehicle
Mians
vehicle
H2O2
Mians
Mians + H2O2
cleaved caspase 3
(% positive cells)
***
###
C
vehicle
AM966
vehicle
H2O2
Mians+H2O2
vehicle
H2O2
Mians+H2O2
cleav
PARP
89 kDa
PARP
116 kDa
vehicle
H2O2
Mians+H2O2
cleav PARP / PARP
(% control)
***
###
###
vehicle
AM966
D
vehicle
H2O2
Mians
Mians+H2O2
cell viability
(% control)
###
#
***
vehicle
AM966
E
vehicle
H2O2
Mians+H2O2
vehicle
AM966
vehicle
H2O2
Mians+H2O2
TUNEL assay
(% positive nuclei)
***
###
###
vehicle
AM966
F
vehicle
H2O2
Mians+H2O2
cell viability
(% control)
#
#
***
vehicle
AM966

Fig. 9